



جامعة الملك عبد الله
للعلوم والتقنية
King Abdullah University of
Science and Technology

Flow Mechanism and Simulation Approaches for Shale Gas Reservoirs: A Review

Item Type	Article
Authors	Zhang, Tao; Sun, Shuyu; Song, Hongqing
Citation	Zhang T, Sun S, Song H (2018) Flow Mechanism and Simulation Approaches for Shale Gas Reservoirs: A Review. Transport in Porous Media. Available: http://dx.doi.org/10.1007/s11242-018-1148-5 .
Eprint version	Post-print
DOI	10.1007/s11242-018-1148-5
Publisher	Springer Nature
Journal	Transport in Porous Media
Rights	Archived with thanks to Transport in Porous Media
Download date	10/08/2022 04:41:27
Link to Item	http://hdl.handle.net/10754/629903

Flow mechanism and simulation approaches for shale gas reservoirs: A review

Tao Zhang¹ Shuyu Sun^{1*} Hongqing Song^{1,2*}

¹Computational Transport Phenomena Laboratory(CTPL), Division of Physical Sciences and Engineering (PSE), King Abdullah University of Science and Technology (KAUST), Thuwal 23955-6900, Kingdom of Saudi Arabia

² School of civil and resource engineering, University of Science and Technology Beijing, 30 Xueyuan Rd, Beijing 100085, People's Republic of China

Abstract

The past two decades have borne remarkable progress in our understanding of flow mechanisms and numerical simulation approaches of shale gas reservoir, with much larger the number of publications in recent five years compared to that before year 2012. In this paper, a review is constructed with three parts: flow mechanism, reservoir models and numerical approaches. In mechanism, it is found that gas adsorption process can be concluded into different isotherm models for various reservoir basins. Multi-component adsorption mechanism are taken into account in recent years. Flow mechanism and equations vary with different Knudsen number, which could be figured out in two ways: Molecular Dynamics (MD) and Lattice Boltzmann Method (LBM). MD has been successfully applied in the study of adsorption, diffusion, displacement and other mechanisms. LBM has been introduced in the study of slippage, Knudsen diffusion and apparent permeability correction. The apparent permeability corrections are introduced to improve classic Darcy's model in matrix with low velocities and fractures with high velocities. At reservoir scale simulation, gas flow models are presented with multiple-porosity classified into organic matrix with nanopores, organic matrix with micropores, inorganic matrix and natural fractures. A popular trend is to incorporate geomechanism with flow model in order to better understand the shale gas production. Finally, to solve the new models based on enhanced flow mechanisms, improved macroscopic numerical approaches, including the finite difference method (FDM) and finite element method (FEM) are common used in this area. Other approaches, like finite volume method (FVM) and fast matching method(FMM) are also developed in recent years.

1. Introduction

Shale gas reservoir is playing an growing important role in the world energy market, due to its significant advantages of less pollution in combustion compared with conventional fuel resources like oil and coal. Starting from the beginning of 21st century

*Corresponding authors: shuyu.sun@kaust.edu.sa, songhongqing@ustb.edu.cn

5 [1–4], shale gas exploitation has become an essential component to bridge the growing
 6 gap between domestic production and consumption and thus secure the energy supply
 7 in North America. [5] The United States successfully became the largest natural gas
 8 producer in 2009, thanks to the high progress in shale gas production. [6, 7] In another
 9 large energy exporter, shale gas resources in Canada are estimated with an amount
 10 larger than 1000 tcf (tera-cubic cubic feet). A paradigm shift has been made toward the
 11 exploration of shale gas in one of the main reservoir block, the Western Canada sedimen-
 12 tary basin (WCSB). [8, 9] With the development and popularity of shale gas exploration
 13 all over the world, there have also been other countries and areas reported with great
 14 potential of exploitation. For example, shale gas resources in China are estimated about
 15 $31 \times 10^{12} m^3$. [10]

16 Properties of shale gas reservoir are essentially needed for successful estimation and
 17 extraction. As a result, accurate characterization and detailed description of reservoirs
 18 should be considered as the prior purpose of relevant researches. Due to the complex
 19 hydraulic and thermal reservoir environment in production, it is hard to reproduce the
 20 same process in laboratory. Thus, numerical simulation has been a popular trend in
 21 the study of unconventional shale gas reservoirs. After a quick investigation on Web
 22 of Science Core Collection , it is found that published papers related with shale gas
 23 numerical simulation has been greatly increased, as shown in Fig.1. A significant increase
 24 could be found from 2012, and continues increasing until now.

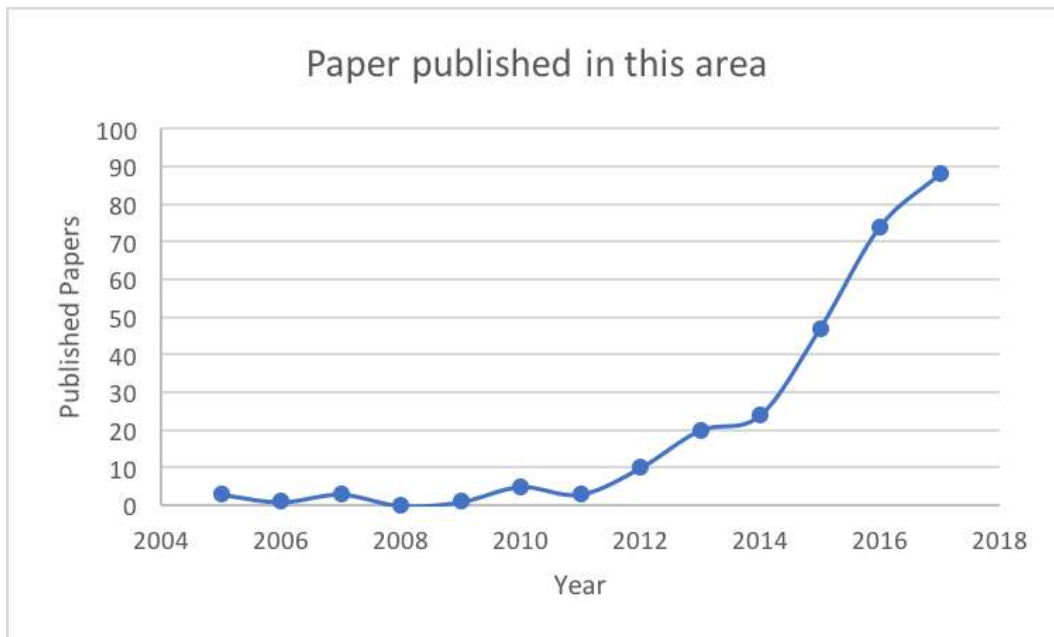


Fig. 1 Paper numbers related with shale gas numerical simulation on Web of Science in recent years

25 This paper is designed to conclude and comment on the flow mechanism and sim-
 26 ulation approaches. First, the adsorption and desorption process is introduced, as
 27 well as the flow regime description. Besides, numerical simulation on micro- and meso-
 28 scales, e.g. molecular dynamics and lattice boltzmann method are reviewed. Mean-

29 while, apparent permeability correction, which is the macroscopic focus, is concluded.
30 Afterwards, we focus on the gas flow simulations at reservoir scales, including numerical
31 models and the effect of geo-mechanics. Finally, the common macroscopic numerical
32 simulation approaches, including finite element method, finite difference method and
33 other schemes, will be presented.

34 **2. Flow mechanism of shale gas**

35 Permeability is always relatively low in shale gas reservoirs, generally less than 1 md,
36 and stratigraphic composition can be divided into different types of intervals (e.g., De-
37 vonian, Jurassic, and Cretaceous strata). [11, 12] The stress-sensitive parameters, in-
38 cluding organic richness, porosity, thickness, and lateral extent can vary significantly
39 with in-situ stress changes. Consequently, the fluid flow and geomechanics impacts are
40 always effected by the change. [13] Such extremely tight rock formations in shale gas
41 reservoirs with different parameters result in the gas transportation occurs through them
42 by different mechanisms. With more efforts been devoted to the researches of such flow
43 mechanisms, the inherent limitations of the conventional macroscopic methods used in
44 petroleum industry are been overcome and new microscopic and mesoscopic approaches
45 including Molecular Dynamics (MD) and Lattice Boltzmann Method (LBM) are intro-
46 duced.

47 **2.1 Adsorption/desorption mechanism**

48 There are three states of gas reserved in shale reservoir: free gas, adsorbed gas and
49 dissolved gas. [14] In previous study, it is found that adsorbed gas is the main state
50 among the above three states, with statistical results indicating that 20% – 80% of the
51 total gas is adsorbed in reservoirs. [15–18] Adsorption properties can provide critical in-
52 formation to help characterize shale structures and optimize hydraulic fracturing. With
53 the decrease of environment pressure, adsorbed gas will become free gas in the early
54 period of exploitation. [19] As a result, gas adsorption/desorption description is of great
55 importance to investigate the well production.

56 Plenties of work have been conducted to study the methane adsorption mechanisms.
57 [20–25] In some studies, molecular accumulation is viewed as the main origin of adsorp-
58 tion on shale surface. It is the consequence of the minimization theory of surface energy.
59 [22] Meanwhile, potential theory is sometimes used to identify the adsorption process,
60 with van der Waals forces leading to physisorption. [24, 25] Besides, properties includ-
61 ing pressure, temperature and geological characteristics have also caused much attention
62 recently on how to affect the adsorption capacity. [22, 23] TOC content, which is short
63 for total organic carbon, is found of high relevance with adsorption capacity. Generally
64 speaking, samples with high TOC content will present high values of contents including
65 total cumulative pore volume, surface area and total porosity, which directly lead to a
66 higher adsorption capacity than the sample with less TOC. Compared with other rocks,

67 shale contains high organic matter, which results in a high gas adsorption amount.

68 Shale permeability will be changed, due to the desorption of gas in the production
69 process. [26] For example, gas desorption process is found in organic grids, known
70 as kerogen, where pressure drop occurs. [27] Meanwhile, pressure difference will be
71 generated between the bulk matrix and the pores, with the pore pressure decreasing in
72 the free gas production process, thus the desorption on the surface of bulk matrix is
73 reinforced.

74 A large number of gas adsorption isotherm models have been proposed in previous
75 studies, such as Langmuir's type model, Freundlich type model, Langmuir-Freundlich
76 type model, D-R type model, BET type model and Toth type models. [28–36]. Most
77 available adsorption models, including their basic equation and the basins where they
78 are applied are listed as Table 1. In this table, V denotes adsorbate volume, P denotes
79 pressure, K denotes an associated equilibrium constant, k denotes Henry's constant, b
80 denotes the adsorption affinity, D denotes the empirical binary-interaction parameter, x
81 and m denotes a constant for a given adsorbate and adsorbent at a particular temperature
82 and c is a constant related to the adsorption net heat. All the subscript L in P_L and V_L
83 denotes the Langmuir pressure and Langmuir volume.

84 Table 1 The comparison of different isotherm adsorption models

Classification	Isotherm model	Basin	Ref
Langmuir	$V = \frac{V_L P}{P_L + P}$	Barnett, the USA	[29, 37]
Freundlich	$V = K p^x$	Mansouri, Iran	[28, 38]
Langmuir-Freundlich	$V = \frac{V_L (bp)^m}{1 + (bp)^m}$	Longmaxi, China	[36, 39, 40]
D-R	$V = V_0 \exp[-D \ln^2(P_s/P)]$	Qaidam, China	[41]
BET	$n_a = \frac{1}{\frac{1}{n_0 c} + \frac{c-1}{n_0 c} \frac{P}{P_0} \frac{P}{P_0} - 1}$	Marcellus, the USA	[30, 42]
Toth	$V = \frac{V_L b p}{[1 + (b p)^k]^{1/k}}$	Bornholm, Denmark	[35, 43]

87 Among the above models, The Langmuir's type model is always considered as the
88 simplest and most effective. [44] With its long history and wide application, model
89 parameters have been reasonably explained and different evaluated models have been
90 proposed based on the original equation. This large set of enhanced models have been
91 used for describing methane and other gas adsorption behaviors with satisfactory per-
92 formance. [45–47] For example, a widely used evaluated form of Langmuir isotherm is
93 given by:

$$q = \frac{\rho_s M_g}{V_{std}} q_a = \frac{\rho_s M_g}{V_{std}} \frac{q_L P}{P_L + P} \quad (1)$$

94 where ρ_s (kg/m^3) denotes the material density of the porous sample, q (kg/m^3) is the
95 mass of gas adsorbed per solid volume, q_a (m^3/kg) is the standard volume of gas ad-
96 sorbed per solid mass, q_L (m^3/kg) is the Langmuir gas volume, V_{std} ($m^3/kmol$) is the
97 molar volume of gas at standard temperature (273.15 K) and pressure (101,325 Pa),
98 p (Pa) is the gas pressure, p_L (Pa) is the Langmuir gas pressure, and M_g (kg/mol) is the
99 molecular weight of gas.

100 In reservoir scale, the effect of gas adsorption capacity are highly extrapolated in
101 regions. As a result, gas in place evaluation and production prediction are quite easy
102 to be overestimated or underestimated and then severely impact the energy industry
103 and social economy. [48, 49] However, the existing models are still in developing and
104 continuous optimization. For example, the original BET model is seldom used at present
105 due to the weak theoretical foundations. It has been found that some assumptions in
106 these models, like multilayer formation, small pore capillary condensation, adsorbed
107 liquid phase and saturation pressure, are no longer suitable for special flow mechanisms
108 of shale gas fluid. [50, 51] Another shortcoming of the classical model is that extrapolated
109 data beyond the test range cannot be fully relied due to different empirical correlations
110 in different temperature regimes. The original physical meanings inside these models,
111 coming from the well-designed experiments, are weakened due to the introduction of
112 some empirical constants. These constants are manually corrected to improve the fitting
113 performance but make the models less reliable. [44] There remains a lot to do to meet
114 the realistic industry conditions better and to help the industry with more accuracy on
115 the production forecast and control.

116 It has been pointed out that gas-in-place volumes in reservoirs are often incorrectly
117 determined for cases with multi-component sorbed gas phase. [52–54] Especially for
118 shale gas fluid flow with high composition of varieties of hydrocarbons (C2+) and sub-
119 sequently high total organic content (TOC), the adjustment of taking multi-component
120 effect into account has been more necessary in the gas-in-place predictions. Compared
121 to conventional approach, the new multi-component model will show a 20 per cent de-
122 crease in total gas storage capacity calculations. [52] Besides, multi-component sorption
123 phenomena, in particular in the primary (micro-) pore structure of the shale matrix, e.g.,
124 co- and counter diffusion and competitive adsorption process are the fundamental inter-
125 ests in the study of CO_2 sequestration and enhanced shale gas recovery. [54] However,
126 the current multi-component adsorption model are still limited on just modifications
127 based on classical single-component Langmuir sorption model. [53, 55] A more uniform
128 and widely applicable model is still in urgent requirement to meet the complex physical
129 and chemical environment of shale gas reservoirs. With the rapid development of fully
130 coupled multi-component multi-continuum compositional simulator which incorporates
131 several transport/storage mechanisms of shale gas reservoirs, a more comprehensive ad-
132 sorption/desorption model is needed to capture and predict the transport process in
133 shale gas reservoirs.

134 **2.2 Flow mechanisms of gas transport in shale gas reservoir**

135 It is important to study the flow mechanism of gas transport in shale gas reservoir.
136 Particular interest have been focused on the multi-scale flow simulation on the sub-
137 surface porous media with pore size ranging from macro-scale ($> 1mm$) to nanoscale
138 ($< 100nm$). [56, 57] Different pore scale characteristics are presented with different flow
139 regimes identified by Knudsen number. [58–61] Slippage and diffusion processes are

140 often viewed as the main flow mechanisms.[62] New approaches, including Molecular
 141 Dynamics (MD) and Lattice Boltzmann Method (LBM), are rapidly developed in these
 142 years to study the flow mechanisms.

143 2.2.1 Flow regime

144 Knudsen number (Kn) is a parameter introduced in gas flow description to identify flow
 145 regimes with different rarefaction degree of gas encountered. Generally, four regimes
 146 are characterized based on Kn : continuous flow ($Kn < 10^{-3}$), slip flow ($10^{-3} < Kn <$
 147 $10^{0.1}$), transition flow ($0.1 < Kn < 10$) and Knudsen flow ($Kn > 10$). [63] Different
 148 interfacial effects are found effective in different flow regimes in small porous structure.
 149 For large tube diameter, the gas flow is mainly viewed as continuous flow with only
 150 slip regime near the wall. [64] Strong interfacial effects are found in shale nanotubes,
 151 which is believed to be caused by two important flow regimes including Knudsen flow
 152 and transitional flow. It should be noted that the flow pattern of single gas flow and
 153 gas-water two phase flow is of big difference. [65] In this paper, we focus on the single
 154 phase flow.

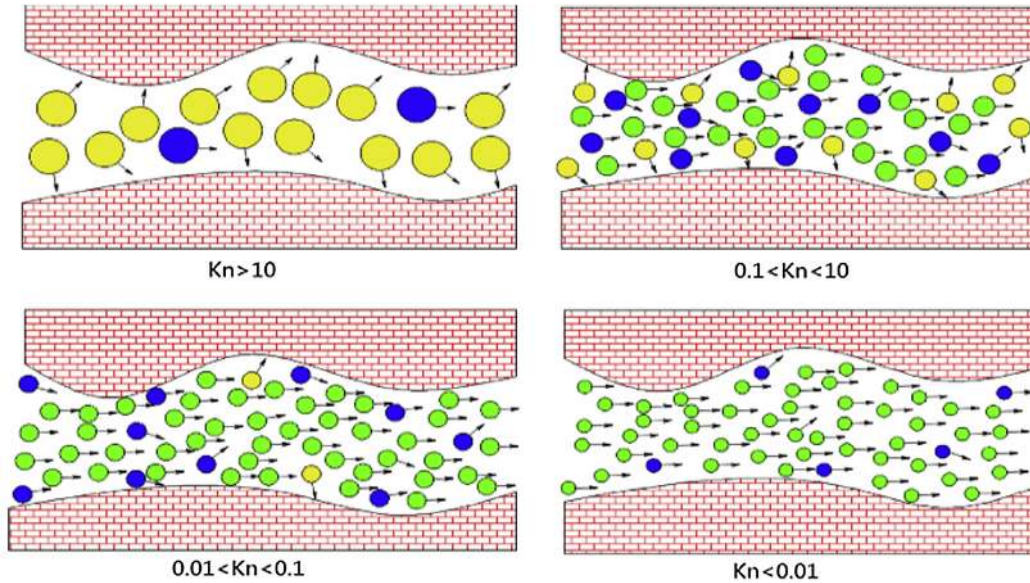


Fig. 2 Schematic diagram of shale gas transport mechanism with different flow regimes[66]

155 A main usage of flow regime characterization is that different governing models,
 156 resulting in different simulation approaches are corresponding to the Knudsen number
 157 and flow regimes. Table 2 shows the gas flow regimes and corresponding governing
 158 equations along with boundary conditions. When Kn varies from 0.001 and 0.1, gas
 159 transportation is in the regime of slip flow, slip boundary condition should be incor-
 160 porated into Navier-Stokes equation or Lattice-Boltzmann method (LBM) to take into
 161 account the slippage on the gas solid interface. When Kn is in a higher range of 0.1
 162 and 10, gas flow enters the transitional regime, where neither Navier-Stokes equation

163 nor lattice-Boltzmann model is applicable any more. Then, Burnett equation based on
 164 higher order moments of Boltzmann equation should be solved or numerical method of
 165 direct simulation Monte Carlo (DSMC) should be used to represent the fluid flow behav-
 166 ior. As Kn goes beyond 10, gas stream is considered as free molecules, and Molecular
 167 Dynamics (MD) must be adopted to capture the physics controlling the gas flow.

168 Table 2 Knudsen number and flow regimes with applicable mathematical models

Particle model	Boltzmann equation (BE)		Collisionless BE	
Continuum model	LBM/NS equation		Molecular Dynamics	
Kn	(0, 0.001)	(0.001, 0.1)	> 10	
Flow regimes	No slip	Slip	Transitional	Free molecular

170 For gas flow in nanotubes, it has been demonstrated that slippage effects will change
 171 the flow regime identification. [67] The concept of slip has a long history, starting from
 172 the famous scientist Navier [68, 69] , and has been used in a large range of practices.
 173 For fluid flow passing rough surface, slip boundary condition is often applied with the
 174 slip-length relevant to roughness height. When $Kn < 10^{-2}$, flow is in continuous regime
 175 and Darcy’s law is enough to describe the flow. As Kn increases from 0.01, diffusive flux
 176 is no longer ignorable and additional term should be considered in the flow equations,
 177 which makes it nonlinear.

178 To correct the permeability with consideration of gas slippage effect, Klinkenberg
 179 approach is often applied in previous studies. [70, 71] For example, to handle flow in all
 180 the four flow regimes, a new equation is proposed in [70, 72, 73], with the gas slip factor
 181 modified based on the dusty-gas model:

$$v = - \left(\frac{D}{p} + \frac{k}{\mu} \right) \nabla p \quad (2)$$

182 A comprehensive model capable of handling gas flow through multi-scale porous me-
 183 dia varying from nanoscale to macro-scale is generated based on the above equation, with
 184 the prospective of molecular kinetics. [74] Knudsen diffusion process is often considered
 185 as driven by collisions of wall with molecule and collective diffusion process is driven
 186 by collision of molecule with molecule. In the new formulation, the collision coefficient
 187 is determined based on the consideration of both Knudsen and collective diffusion. It is
 188 figured out that for single phase fluid flow in nanotubes, the interfacial effects existed in
 189 the wall surface will lead to form a thin liquid film and the flow characteristics will be
 190 changed then. [75] The stress singularity is removed in thin film theory, and fluid front
 191 is thought to move over dry surface. It has been shown in previous simulations that
 192 separations of about ten molecular diameters down will be resulted in the fluid viscosity
 193 with the bulk value. [68] There has also been assumptions [76, 77] that the formed gas
 194 film has a thickness between the molecular size and the gas mean free path. Molecular
 195 dynamics simulation has proved that Myer’s model is correct. [78]

196 Geometrical properties of fractured porous media is vital to predict and evaluate
 197 the hydraulic transport properties of fracture networks. [79, 80] Although a variety of

198 subjects have been studied related to geometrical, fractal and hydraulic properties of
199 fractured porous media such as rock masses and reservoirs, a gap still exists between
200 theoretical knowledge and field practice. [81] It is of great importance to seek new
201 theoretical and numerical studies and advances in various subjects addressing flow and
202 transport mechanism as well as hydrocarbon recovery improvement, such as innovative
203 stimulation techniques, reservoir characterization, and other approaches. Specifically,
204 not all the length distribution of fractures and fracture networks are follows the fractal
205 law. They may be multi-fractal, and even non-fractal. Thus, more elaborate explorations
206 are need for adequately characterizing the complex fractured networks. As we discussed
207 in above section, fractal dimension is one of most important parameters to quantitatively
208 characterize the complexity of fractures. However, fractal dimension is sensitive to
209 prediction methods, even some irrational values may be obtained. [82] Future works also
210 should be focused on the influence of fracture surface roughness, hydraulic gradient, the
211 coupled thermo-hydro-mechanical-chemical processes.

212 **2.2.2 Molecular dynamics for shale gas transportation**

213 Molecular dynamics (MD) simulation approaches recognize the fluid flow as a swarm of
214 discrete particles and is suitable for flow simulation with high Kn number. It is often seen
215 as an accurate approach due to the deterministic [83] or probabilistic [84] calculation of
216 the particle properties at every time steps. [83, 85, 86] These properties include particle
217 inertia, position and state. Boltzmann distribution is often used to describe individual
218 particle dynamics at different temperatures. Newton's equation of motion is integrated
219 numerically to determine the two-body potential energy and transient evaluation of two
220 particles and then to find the particle positions.

221 A general purpose of using MD simulation is to investigate the adsorption and desorp-
222 tion (displacement) process of shale gas flow. [87–89] Some researchers have performed
223 numerous studies using molecular dynamic simulations to model gas flow through a sin-
224 gle nanotube, in which the interface microstructure phenomenon is of special interest
225 [90]. The results have shown that the interactions between fluid and solid wall is a great
226 cause of flow promotion. Meanwhile, MD studies have been performed to understand
227 the shale gas diffusion process in special pores [91] and study thermodynamical prop-
228 erties of gas transport in montmorillonite (MMT). [92, 93] MD studies are also carried
229 out to help describe the pore structures in shale formations [94] and it can also be used
230 in the general gas recovery process. [95] In Table 3, we listed five recent papers with
231 high citing rates relevant to molecular dynamics simulation of shale gas reservoirs. [The](#)
232 [citations of each paper is searched from Web of Science Core Database.](#)

233 Table 3 Five high-citing papers of MD simulation of shale gas reservoirs

Authors	Year	Interest	Ref	Cited by
Sharma, et al	2015	Adsorption/Diffusion	[87]	35
Zhehui, et al	2015	Molecular velocity in nanopores	[88]	22
HengAn, et al	2015	Adsorption/Displacement	[89]	30
Mahnaz, et al	2014	Pore size distribution	[94]	49
Quanzi , et al	2015	Enhanced recovery	[95]	26

235 It should be noted that, modern computation capability, represented by supercom-
236 puters, is still not enough to handle a reasonable, practical and very detailed flow simu-
237 lation through nanotubes network in time and space scale of the real production process
238 in shale gas reservoir. Although MD models are designed to capture microscopic inter-
239 actions, which is the foundation of macroscopic phenomenons, time steps are generally
240 strictly limited to femtoseconds (10^{-15} s), which results in the limitation of simulation
241 time scale generally ranging from picoseconds (10^{-12} s) to nanoseconds (10^{-9} s). [83]

242 2.2.3 Lattice Boltzmann Method

243 The Lattice Boltzmann Method (LBM) has been proved to be a useful and efficient
244 approach to study the shale gas reservoirs. [96, 97] Knudsen diffusion has already been
245 incorporated in the general LBM flow models to describe transport properties of shale gas
246 fluid flows. [96] For multiphase flow, the famous Shan–Chen model of single-component
247 multiphase flow is common used. [97]

248 The first attempt to take Knudsen diffusion into account of the fluid flow using
249 LBM simulation approach is said to be in [97]. In their study, compared to common
250 used shale tortuosity, which is an important component of Bruggeman equation, the im-
251 proved model will lead to a much higher tortuosity result and consequently the intrinsic
252 permeability is said to be extremely lower. [97] For relative permeability, it is found that
253 the countercurrent relative permeabilities, as a function of wetting saturations, usually
254 seem smaller than the cocurrent ones with a Lattice Boltzmann scheme derived for two
255 phase steady-state flow. [98]

256 Characteristics of gas flow in organic nano-pores in shale gas reservoirs can be evalu-
257 ated effectively using developed LBM simulation. Under assumptions of small Knudsen
258 number, flow properties simulated with LBM models agree well with the classical macro-
259 scopic Poiseuille’s law. Flow capacity, or flow rate, is found to be proportional to the
260 square of pore size. [96] However, the relaxation time used in LBM models should be
261 corrected to cover simulations at high Kn value. Permeability is increased as the result
262 of velocity enhancement caused by slippage effect on pore walls. Adsorptive and cohesive
263 forces among particles in gas fluid flow is used to simulate molecular level interactions
264 accounting with LBM scheme in [99]. With slip boundary condition of Langmuir type at
265 organic pore walls, mass transport along the tube walls is partitioned into two compo-
266 nents: hopping of adsorbed gas molecules and slippage of free gas molecules. Hopping is
267 the process of surface transport. In Table 4, we listed five recent papers with high citing

268 rates relevant to lattice boltzmann simulation of shale gas reservoirs. The citations of
 269 each paper is searched from Web of Science Core Database.

270 Table 4 Five high-citing papers of LBM simulation of shale gas reservoirs

Authors	Year	Interest	Ref	Cited by
Chen, et al	2015	Knudsen diffusion	[97]	70
Fathi, et al	2012	Slippage and hopping	[99]	24
XIaoling, et al	2014	Apparent permeability	[96]	31
Ebrahim, et al	2012	Klinkenberg effect	[100]	58
Song, et al	2015	Gas flow rate	[101]	13

272 Previous researches have shown that approaches belonging to Lattice Boltzmann
 273 scheme are still limited in the application of rapidly recovering the imaging of pore
 274 structure and furthermore in the simulaiton and visulization of fluid flow in porous
 275 media, especially less effective in 3 dimensions. Pore-network models, which is also
 276 a meso-scopic approach, is capable of simplifying detailed large scale pore structures
 277 into a readable network constituting of pore bodies connected by pore throats. [102–
 278 105] Each pore body is associated with different number of attributes, which is called
 279 coordinates numbers, and the spatial location is then specified explicitly. In this way,
 280 the highly irregular porous space is reduced to a network with topology and geometry
 281 easy captured. [4]

282 2.3 Apparent permeability correction

283 A standard approach to study gas transpotation in porous media is the famous Darcy’s
 284 law. [106] In this theory, the average macroscopic gas velocity v is assumed to be
 285 determined by global permeability k and the pressure gradient ∇p across the media

$$v = -\frac{k}{\mu}\nabla p \quad (3)$$

286 where μ is the gas viscosity. The permeability k is a macroscopic parameter defined to
 287 describe the relation between gas flow and pore structure. Same as many other classical
 288 macroscopic theories, Darcy’s law was first concluded from experiments conducted by
 289 Darcy [106]. It is proved that Darcy’s law can also be derived from Navier-Stokes
 290 equation as a simplification and extension in porous media. [70].

291 However, the long history research of shale gas reservoir have brought insights of
 292 special percolation characteristics and flow mechanisms in the tight rock structures.
 293 The original Darcy’s equation is no longer capable of explaining these phenomenons.
 294 A strict limitation of flow velocity is found in the application of classical Darcy’s law.
 295 For highly fractured reservoir structures, gas flow is at relatively high velocity and the
 296 original Darcy’s law will lead to misleading results, sometimes with an over prediction
 297 of productivity as much as 100%. [107] To facilitate the inclusion of this phenomenon
 298 into reservoir simulators, many multipliers are generated to correlate the apparent per-
 299 meability to the absolute permeability in different flow regimes.

300 Experimental studies on permeability enhancement effects in tight formations date
 301 back to the early 20th century. In 1941, based on gas flooding experiments, Klinkenberg
 302 [108] proposed a correlation equation of the apparent gas permeability k_a to the absolute
 303 permeability k_∞ via

$$k_a = \left(1 + \frac{b}{p}\right) k_\infty \quad (4)$$

304 where b is the Klinkenberg factor and p represents average pressure across the core. The
 305 Klinkenberg factor is usually obtained by matching experimental data. Klinkenberg's
 306 correction can be applied in the low Knudsen number range (< 0.1), therefore it is widely
 307 adopted for simulating low permeability gas reservoirs. The Klinkenberg factor is often
 308 calculated by a function of the absolute permeability and the rock porosity. Different
 309 expressions of Klinkenberg factor b can be found in [109–111].

310 So far, no satisfactory apparent permeability correction has been developed for the
 311 transitional flow regime due to its complexity. A widely accepted correlation equation is
 312 proposed in 1999 by Beskok [112], with the multiplier relevant to Kn , and many other
 313 correlations have been developed based on it,

$$K = K_\infty f(Kn) \quad (5)$$

314 In the above equation, $f(Kn)$ is a flow condition function given as a function of the
 315 Knudsen number Kn , the dimensionless rarefaction coefficient α , and the slip coefficient
 316 b , which is an empirical parameter, by:

$$f(Kn) = (1 + \alpha Kn) \left(1 + \frac{4Kn}{1 - bKn}\right) \quad (6)$$

317 The most important parameter is the slip coefficient, which is described as "the vor-
 318 ticity flux into the surface divided by the vorticity of flow field on the surface, obtained
 319 by the no-slip approximation". [63] To obtain the value, direct simulation Monte Carlo
 320 (DSMC) method or linearized Boltzmann equation are the two main approaches com-
 321 monly used and sometimes laboratory experiments are designed for this. Slippage effects
 322 are enhanced at low pressure condition and the adsorption layer thickness is reduced,
 323 which results in a larger coefficient measured at ambient condition experiments. [113]
 324 The linearity property of Darcy's law is broken as the permeability increases. A new
 325 developed model of Beskok type scheme to calculate multiplier is proposed recently as
 326 [113]

$$f(K_n) = \begin{cases} 1 + 5K_n & \text{Slip Regime} \\ 0.8453 + 5.4576K_n + 0.1633K_n^2 & \text{Transition Regime} \end{cases} \quad (7)$$

327 Within the free molecular or Knudsen flow regime, the apparent gas permeability
 328 can be calculated by considering the diffusivity for Knudsen diffusion from gas kinetics.

$$D = \frac{1}{3}du = \frac{1}{3}d\sqrt{\frac{8RT}{\pi M_A}} \quad (8)$$

329 where u is gas molecules thermal velocity, R is the gas constant, and M_A is the gas
 330 molecular weight. The derivation of Knudsen diffusion coefficient can be found in [114].
 331 By rearranging the above equation, we can get an apparent gas permeability formulation
 332 similar to the Klinkenberg's correlation:

$$k_a = \left(1 + \frac{b}{p}\right) k_\infty \quad (9)$$

333 where $b_a = pc_g\mu_g D/k_\infty$. [115]

334 Slip flow, transition diffusion and surface diffusion are incorporated in a flux model
 335 proposed in 2017 [116], and the apparent permeability is derived as:

$$k_{app} = \frac{Fr^2}{8} + \frac{\mu D_T}{p} + \frac{\mu D_s \varsigma_{ms} R T C_s}{p^2} \quad (10)$$

336 In table 5, we listed different types of apparent permeability correction models that
 337 have been proposed. It is noted that Sun's model is a developed model based on classical
 338 Klinkenberg equation, which is proved with better accuracy. [115]

339 Table 5 Comparison of different apparent permeability correction models

Model	Equation	Regime	Ref
Klinkenberg	$k_a = \left(1 + \frac{b}{p}\right) k_\infty$	Low Knudsen number	[108]
Beskok	$f(Kn) = (1 + \alpha Kn) \left(1 + \frac{4Kn}{1-bKn}\right)$	Transitional flow	[112]
Pour	$f(K_n) = \begin{cases} 1 + 5K_n \\ 0.8453 + 5.4576K_n + 0.1633K_n^2 \end{cases}$	Transitional flow	[113]
Sun	$k_a = \left(1 + \frac{b_\alpha}{p}\right) k_\infty$	free molecular flow	[115]
He	$k_{app} = \frac{Fr^2}{8} + \frac{\mu D_T}{p} + \frac{\mu D_s \varsigma_{ms} R T C_s}{p^2}$	free molecular flow	[116]

342 2.4 Improved Darcy model in fractures

343 It is important to modify original Darcy's equation to consider turbulent flow pattern
 344 of the gas transport in shale fractures where the inertial forces are relatively high. [117]
 345 Forchheimer equation is a common used formula to describe non-Darcy flow. It is ob-
 346 served that the linear relationship between the fluid velocity and pressure gradient in
 347 traditional Darcy's law is no longer valid at high flow rates. The non-Darcy flow coeffi-
 348 cient, β , is then defined as a secondary proportional constant in addition to the perme-
 349 ability k to introduce the nonlinearity. The improved model with the two coefficients
 350 can be written as

$$-\frac{dp}{dx} = \frac{\mu v}{k} + \beta \rho v^2 \quad (11)$$

351 Non-Darcy coefficient β is of growing interest as it can be easily used in reservoir
 352 simulation. [118] Many theoretical correlations have been developed to calculate this
 353 parameter. A comprehensive model derived from experimental data is applied in nu-
 354 merical simulation, which is proved to be valid for single phase gas flow in porous media

355 belonging to all ranges of flow regimes. [119] A parallel and serial two-type model is pro-
 356 posed to describe the porous structure. [120] In this classification, the porous medium is
 357 assumed to be made up of straight bundle and parallel capillaries with uniform diameter
 358 in parallel type. The serial type is assumed to the structure serially lined pore space.
 359 For both the two models, non-Darcy coefficient β is given as

$$\beta = \frac{c}{K^{0.5}\phi^{1.5}} \text{ Parallel type model} \quad (12)$$

360 It is found that the above equation with additional quadratic term of velocity is
 361 limited within certain range of data set. [121] To handle deviations, another cubic term
 362 of velocity is introduced to better meet all data set:

$$-\frac{\partial p}{\partial x} = \frac{\mu v}{k} + \beta \rho v^2 + \gamma \rho v^3 \quad (13)$$

363 However, the above Forchheimer cubic equation with constant β and γ parameters
 364 still not meet all the data set very well. Apparent permeability is observed to be larger
 365 than predictions using Forchheimer type equations at high flow rate. Based on extensive
 366 laboratory and field experimental data sets, a new and more general model, which is
 367 known as Barree and Conway model [12], is proposed in 2004 to overcome the problems
 368 caused by constant β and γ values. Darcy's law is again valid in the Barree and Conway
 369 model, with apparent permeability:

$$-\frac{\partial p}{\partial L} = \frac{\mu v}{k_{app}} \quad (14)$$

370 Barree and Conway model is proved to address the discrepancies, which may cause
 371 significant impact on the relationship between pressure and flow rate distribution in
 372 porous media. [122] As shown in Fig. 3, the Barree and Conway model meets much
 373 better with the experimental data of pressure drop and flow rate, while Forchheimer
 374 quadratic equation will overestimate the pressure drop at high flow rate but Forchheimer
 375 cubic equation underestimate the pressure drop.

376 The Barree and Conway model (BCM) has widely applied in modern petroleum
 377 industry as a basic mathematical model of shale gas reservoir simulator. A 3D single
 378 phase fluid flow scheme is derived according to Forchheimer and BCM equations to
 379 simulate pressure transient analysis in fractured reservoirs. [123] Combining both the
 380 two equations, an equivalent non-Darcy flow coefficient can be calculated to describe all
 381 non-Darcy flow phenomena coupling with near-wellbore effects. Besides, the BCM has
 382 already been extended to model the multiphase flow in porous media, which is widely
 383 used in practical shale gas reservoir simulator. [124]

384 The recent development of shale gas reservoir simulation techniques has witnessed new
 385 evolutions based on Barree and Conway model. Barree [125] improved this model with
 386 no more assumptions of a constant permeability or a constant β . In the new model,
 387 correlations of pressure drop and flow velocity can be valid for the whole porous media
 388 [126]:

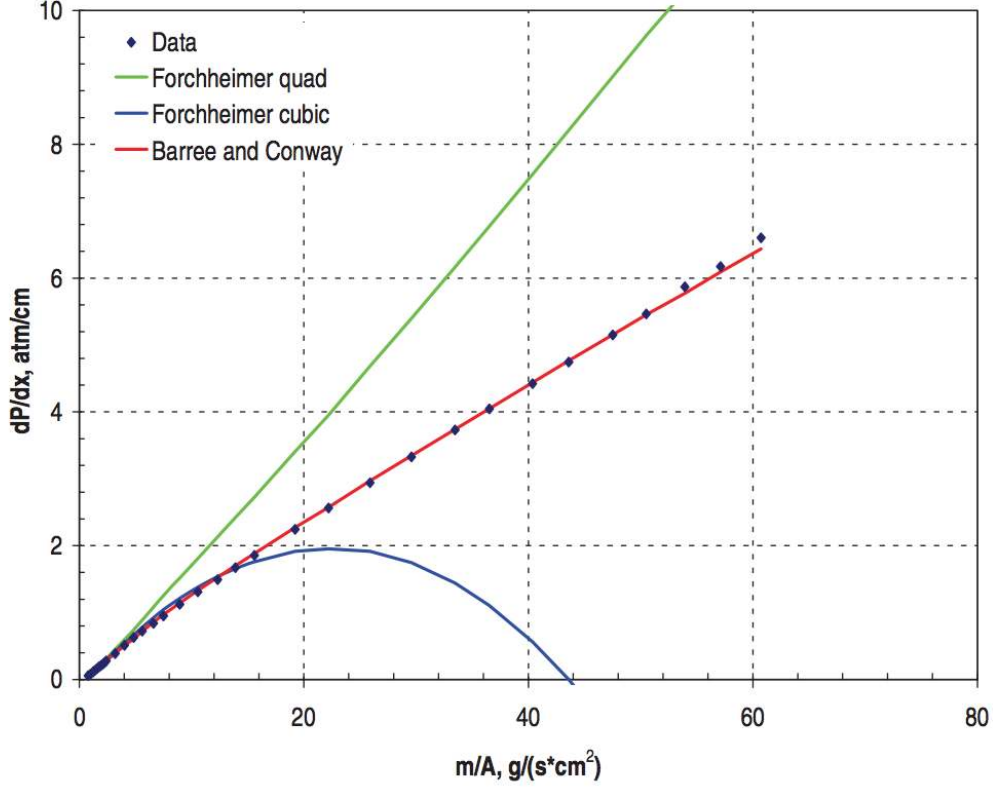


Fig. 3 The comparison between pressure gradient and mass flow rate under certain condition with different models[122]

$$\frac{\partial p}{\partial L} = \mu v / k_d \left[k_{mr} + \frac{(1 + k_{mr})}{\left(1 + \frac{\rho v}{\mu T}\right)} \right] \quad (15)$$

389 3. Gas flow simulation at reservoir scale

390 3.1 Flow models

391 Shale is generally viewed as sediments with very fine grains and obvious fissility. [127].
 392 The porous media, constituting of pores with diameters ranging from nanometer to
 393 micrometer, is classified into inter-particle and intra-particle pores. The intra-particle
 394 pores are associated with organic matter pores within kerogen and mineral particles
 395 [128].

396 Different physical properties has been illustrated in the organic matter pore com-
 397 pared with rock constituents common seen. The special properties play significantly
 398 impact on the gas storage and flow in shale. Numerous small pores are found in larger
 399 pores residing on their interior walls in kerogen. [129] Besides, cross section of pores
 400 in kerogen are observed to be round. Kerogen is also thought to be the place where
 401 gas adsorb on the wall and dissolve within it. [127, 130] The pore structure in organic
 402 matter is generally considered as gas-wetting due to it is formed in hydrocarbon gen-

403 eration process. [131, 132] As the organic matter is so unique with these features, a
 404 four type classification of organic-rich shale structure is common accepted, where the
 405 porosity systems are divided into hydraulic fracture, natural fractures, kerogen (organic
 406 matrix) and inorganic matter the pore size decreasing [132], as shown in Fig. 4. Another
 407 classification approach is to categorize the shale reservoir into four different pore systems
 408 as organic porosity, inorganic porosity, natural fractures, and hydraulic fractures. [133]

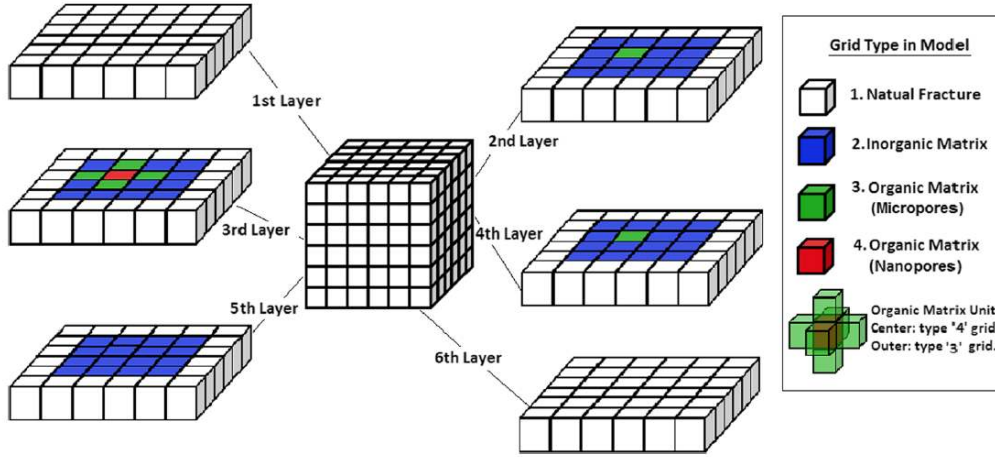


Fig. 4 Schematic of micro-scale model: a grid system for instance, with one organic matrix unit randomly distributed in shale matrix core surrounded by natural fracture grid[134]

409 Different approaches have been developed to capture the shale properties in reservoir
 410 simulations. Multiple interacting continua (MINC) and explicit fracture modeling are
 411 proposed to generate an efficient scheme with single porosity for shale gas simulation.
 412 [135] A coarse-grid model incorporating numerical dynamic skin factor is presented for
 413 shale reservoirs with hydraulic fractures. [136] To handle practical well performance in
 414 a long term as well as common transient behavior, the coarse-grid model is improved to
 415 better describe the fractures and wells. [137]

416 For different connections in organic matters with different pore sizes, free gas flow
 417 mechanism varies. Generally speaking, for connections between nano-pores and micro-
 418 pores in organic matter, only Fickian diffusion is the driven of desorbed gas flow. For
 419 connections between micro-pores in organic matters, both Darcy's law and Fickian dif-
 420 fusion should be considered. For other connections, Darcy's law is often assumed to be
 421 the only driven force. A general mass conservation equation is derived to accommodate
 422 all the three assumptions and describe a single-component and single-phase isothermal
 423 flow system [134]:

$$\nabla \cdot \left[\rho_g \left(D_f C_g \nabla P + \frac{K}{\mu_g} (\nabla p + \rho_g g \nabla z) \right) \right] = - \left[\frac{\partial (\rho_g \varphi)}{\partial t} + \frac{\partial (q_a (1 - \varphi))}{\partial t} \right] \quad (16)$$

424 where D_f is the Fickian diffusion coefficient, C_g is the gas permeability, μ_g is the gas
 425 viscosity, K is the media permeability, q_a is the mass of gas adsorbed on unit volume of

426 media and φ is the porosity of the porous media. The first term on the left hand side
 427 of above equation represents the Fickian diffusion flux, the second term represents the
 428 Darcy flow flux. On the right hand side, the first term refers to the compressed gas in
 429 all the grids and the second term refers to the accumulation of desorbed gas in organic
 430 grid blocks.

431 Darcy’s law is quite limited in shale matrix as the permeability is extremely low
 432 there. As a result, many innovative methods have been proposed to investigate the flow
 433 mechanisms instead of dual-permeability and dual porosity models common used in
 434 conventional oil and gas reservoirs. One approach is called the dual-mechanism model,
 435 which considers both the Fickian diffusion and Darcy flow, and dynamic gas slippage
 436 factor is introduced to describe the gas flow in tight formations. [138, 139] Another
 437 method is proposed in 2012 [140], using a flow condition function of Knudsen number
 438 to correct apparent permeability with intrinsic permeability. However, further confir-
 439 mation is still needed to validate the suitability to various flow regimes. An improved
 440 multiple-porosity model is recently developed [134], where several porosity systems are
 441 tied through arbitrary connectivities against each other, as shown in Fig. 5. It is il-
 442 lustrated that upscaling techniques can be used to extend this model to shale gas flow
 443 simulation at reservoir scale with complex mechanisms.

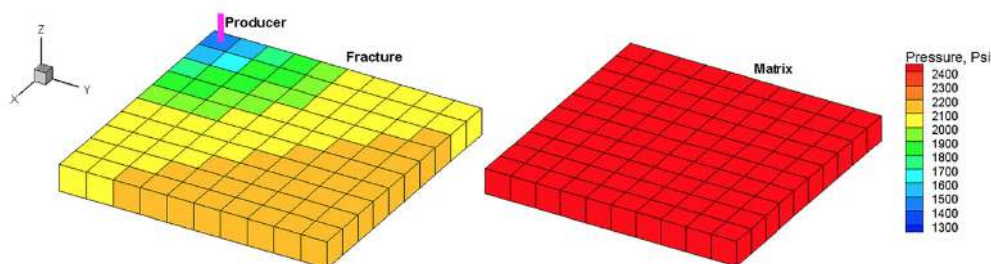


Fig. 5 Dual-porosity model used for validation of variable permeability, left map:
 fracture; right map: matrix[134]

444 3.2 Flow model coupled with geomechanics

445 Geomechanics is of critical importance to be incorporated in the reservoir simulation to
 446 better describe the underground pressure and velocity distribution. An efficient and reli-
 447 able prediction on hydrocarbon production is closely relevant to an accurate description
 448 of rock physics which might be changed by field operations.

449 Due to the complex rock characteristics in shale gas reservoirs, geological conditions
 450 are hard to depict and model with conventional methods. [141] After a quick review
 451 on previous studies coupling geomechanics and flow models in shale gas reservoirs, two
 452 classifications are concluded with different focus. Some researches are concentrated on
 453 the improvement of model accuracy, efficiency and reliability. [142–146] Iterative meth-
 454 ods are developed [142], space discretization is optimized [143] and solution convergence
 455 is improved. [144] Meanwhile, practical applications of coupled models on shale gas

456 reservoir exploration processes are discussed. [147, 148] Effects of plasticity on produc-
 457 tion performance is taken into account [147] and the difference of introducing responses
 458 to field operations is demonstrated. [148] A well-established flow model coupled with
 459 geomechanics is proposed recently to examine the effects of hydraulic fracture geometry
 460 and rock mechanics on hydrocarbon production and pressure distribution in unconven-
 461 tional reservoirs. The fully coupled numerical model is validated with an analytical
 462 solution and used to history match with field data. This model has been proved to be
 463 successful in the investigation of reservoir performance and in the characterization of the
 464 pressure distribution in cases with various rock elastic properties and hydraulic fracture
 465 designs. [149]:

$$\rho_g \left[\frac{\alpha - \phi}{K_s} + \phi \frac{M_g}{RT\rho_g} \left(\frac{1}{z_g} - \frac{p}{z_g^2} \frac{\partial z_g}{\partial p_g} \right) \right] \frac{\partial p_g}{\partial t} + \rho_g \alpha \frac{\partial e_v}{\partial t} + \nabla \cdot (\rho_g v) = \rho_g q_g \quad (17)$$

$$\nabla \cdot [\sigma_0 + \lambda tr(\varepsilon) I + 2\mu\varepsilon - \alpha(p - p_0) I] = 0 \quad (18)$$

466 where z_g is the real gas factor, M_g is the gas molar mass, R is the gas constant, T is
 467 the absolute temperature, α is the Biot's coefficient, σ_0 is the initial total stress tensor,
 468 λ is the first Lamé's constant, μ is the second Lamé's constant and $tr(\varepsilon)$ is the trace of
 469 strain tensor.

470 Necessary properties needed for production workflow, like pressure and deformation
 471 process, can be better provided from the coupling models. [150] It is found in previous
 472 research [151] that gas production will be overestimated if geomechanics is not incor-
 473 porated in the flow models. The production rate in naturally fractured reservoirs is
 474 proved to be highly sensitive to fracture aperture changes. [152] With the introducing
 475 of stress sensitivity, well production will be reduced. The effect of total organic carbon
 476 (TOC) on gas production is studied with a model coupling geomechanics and flow, and
 477 the cumulative production is said to be increased if TOC is larger. [153]

478 Generally, only linear elasticity is considered in geomechanics numerical model, which
 479 leads to the disability of recovering nonlinear elastic behaviors caused by hydrocarbon
 480 depletion and stress changes in shale gas reservoirs. [153, 154] To handle this problem,
 481 an enhanced coupling model is proposed recently to consider nonlinear elasticity. [155]
 482 It is found that as rocks are being compacted and consolidated during the production
 483 process, permeability values are quite different and meet experiment data better than
 484 linear elasticity models on samples obtained from the Longmaxi Formation in China.
 485 It is indicated that permeability will be overestimated by 1.6 to 53 time if nonlinear
 486 elasticity is not considered.

487 4. Macroscopic numerical simulation approaches

488 Analytical methods are not capable of solving the mathematical formulas constituting
 489 flow models of shale gas reservoirs. As a result, numerical methods are strongly needed
 490 to solve the model. In petroleum industry, numerical simulations can go back to 1950s,

491 and now have been applied in a wide range of complex fluid flow processes. Except for
492 microscopic and mesoscopic approaches discussed in Section 2, macroscopic approaches
493 are also common methods to provide numerical solutions of fluid flow in shale gas reser-
494 voirs. Due to the long history of the application, some macroscopic approaches, like finite
495 difference method (FDM) and finite element method (FEM) are more common used and
496 well developed. Recently, efforts have also been paid on other methods including finite
497 volume method (FVM) and fast matching method(FMM).

498 **4.1 Finite Difference Method**

499 In reservoir simulation, and even larger scale of flow simulation, FDM is always viewed
500 as the most commonly used and best developed method. Discretization of ordinary and
501 partial differential equations modeling flow in reservoirs are the first procedure in the
502 technique. Afterwards, a finite difference grid should be constructed on the simulated
503 reservoir area and the method implementation is conducted on the grids. For boundary
504 conditions, pressure information is common used at each boundary point at the block.
505 [156] It is found that the accuracy of numerical results using finite difference methods
506 is deeply relevant to the grid division and boundary conditions. [157] Truncations on
507 Taylor series expansion are used to solve unknown velocity and pressure distribution
508 with spatial derivatives. [158]

509 The main advantage of FDM over FEM is the efficiency and simplicity. Rectangular
510 and triangular grids, uniform and non-uniform meshes, Cartesian and curvilinear coord-
511 inates have all been proved to be easy to implement in reservoir simulations extended
512 from 1D to 3D. Especially for 3D complex flow problems, FDM is said to be far superior,
513 although problems like numerical dispersion and grid dependence may occur.[159]

514 **4.2 Finite Element Method**

515 Compared to FDM, FEM is said to be more accurate in reservoir simulations. Opposed
516 to piecewise constant approximation, FDM results in a linear approximation solution.
517 [160] Besides, the flexibility of accommodations to unstructured meshes is demonstrated
518 in studies using FEM. As a result, FEM is more capable of describing flow properties in
519 complex porous structures in reservoir geometry from fracture to matrix, and excellent
520 efficiency could still be preserved. [160, 161]

521 Complex rock structures in special geometry of shale gas formations, such as non-
522 planar and non-orthogonal fractures, make Cartesian grids inadequate to be used in shale
523 gas reservoir simulation using FEM. Thus, unstructured meshing is required to capture
524 the fracture geometry. [162] Starting from 1979 [163], unstructured meshing skills have
525 been widely used and extended to incorporations with local grid refinement. [157, 164]
526 A new compositional model based on unstructured PEBI (perpendicular bisector) is
527 proposed in 2015 [165] to characterize the properties of non-Darcy flow in a wide range
528 of slip, transitional and free molecular flow regimes and multi-component adsorption

529 processes. Although much time and effort should be paid on the grids generation,
 530 the advantages of unstructured meshing skills are still worthwhile. Complex boundary
 531 conditions such as pinch out and faults can be represented much more easily and local
 532 refinement is more flexible. To orient grids when needed, it is easier as well compared
 533 to structured grids. The improvement of accuracy by unstructured grids is proved
 534 in previous studies [166], as well as CPU performance. An example of two kinds of
 535 unstructured is illustrated in Fig. 6.

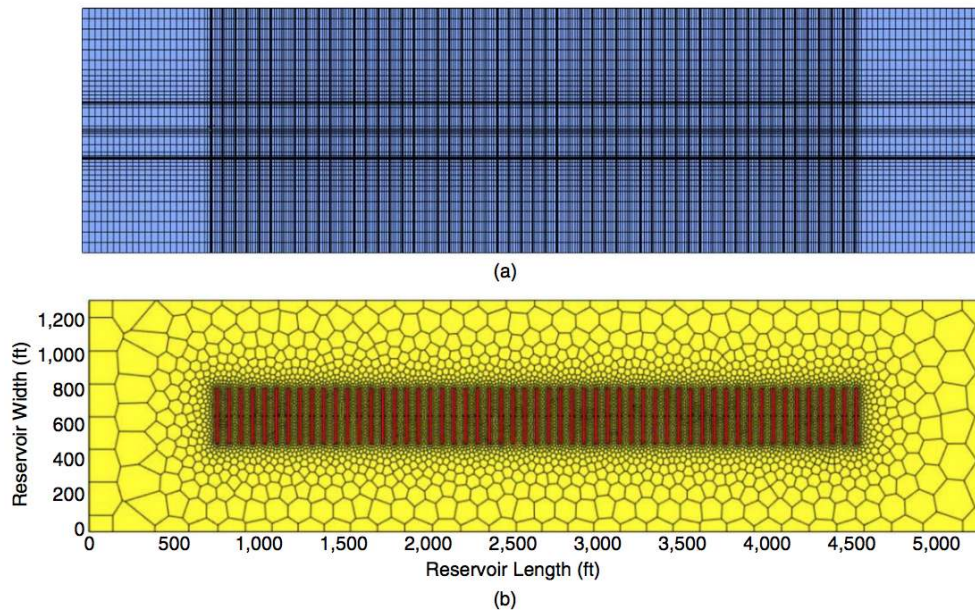


Fig. 6 The comparison between (a) the tartan grid and (b) the PEBI grid for 2D synthetic model[166]

536 Upscaling or homogenization techniques are widely used in traditional researches to
 537 develop effective parameters that represent subscale behavior in an averaged sense on a
 538 coarser scale as flow modeling needs to be concerned on a wide range of spatial and tem-
 539 poral scales in practical reservoir simulation. [167–170] In an attempt to overcome some
 540 of the limitations of upscaling methods, so-called multiscale discretization methods have
 541 been proposed over the past two decades to solve second-order elliptic equations with
 542 strongly heterogeneous coefficients[171]. This includes methods such as the generalized
 543 finite-element methods [172], numerical-subgrid upscaling [173], multiscale mixed finite-
 544 element methods [174] and mortar mixed finite-element methods. [175] The key idea
 545 of all these methods is to construct a set of prolongation operators (or basis functions)
 546 that map between unknowns associated with cells of the fine geo-cellular grid and un-
 547 knowns on a coarser grid used for dynamic simulation. Over the past decade, there have
 548 primarily been main developments in this direction focusing on the multiscale mixed
 549 finite-element (MsMFE) method. The main process is to make this method as geomet-
 550 rically flexible as possible and developing coarsening strategies that semi-automatically
 551 adapt to barriers, channels, faults, and wells in a way that ensures good accuracy for a
 552 chosen level of coarsening. In order to produce high-quality approximate solutions for

553 complex industry-standard grids with high aspect ratios and unstructured connections,
554 a new multiscale formulation has been presented recently [176], which could guarantee
555 the robustness, accuracy, flexibility as well as simplification on the implementation. Be-
556 sides, many works have been done on the weighted Jacobi smoothing on interpolation
557 operators with a large degree of success in the algebraic multigrid (AMG) community
558 where fast coarsening is combined with simple operators constructed via one or two
559 smoothing steps [177–179] as an inexpensive alternative to the interpolation operators
560 used in standard AMG [180]. Many high performance multigrid solvers have been pro-
561 posed to support smoothed aggregation as a strategy for large, complex problems [181]
562 due to the inexpensive coarsening and interpolation strategies.

563 4.3 Other Methods

564 For reservoir simulations incorporating complex rock geometries, finite volume method
565 (FVM) is said to be more easily implemented with unstructured grids. It is a fairly
566 new developed technique and mainly focusing on discretization methodologies. [182] It
567 is proved that to get numerical approximations at the same level of accuracy, FVM is
568 easier and faster compared to FEM. Compared to FDM, FVM is believed to have better
569 versatility.

570 Another comprehensive approach in shale gas reservoir simulation is a class of front-
571 tracking methods called fast marching method (FMM). [183–186] The well-drainage
572 volume can be computed efficiently using this method, where the propagation equation
573 (Eikonal equation [187] is directly solved of a maximum impulse response. [188] FMM is
574 proved to be very efficient in solving the Eikonal equation, where CPU times are only in
575 seconds level but other comparable methods need hours. Besides the close corresponding
576 with the analytic solution, the common front resolution problems are also solved. [189]
577 Fig. 7 shows two illustrative examples using FMM method with unstructured triangular
578 grids.

579 5. Conclusion

580 This paper reviews the flow mechanism and numerical simulation approaches of shale
581 gas reservoirs. Investigation of gas adsorption/desorption is important to predict well
582 production, and gas adsorption isotherm can be concluded into different models. With
583 the classification of flow regimes based on Knudsen number, different governing equa-
584 tions and numerical approaches are suitable for different gas transport mechanism. Mi-
585 croscopic and mesoscopic approaches, represented by Molecular Dynamics (MD) and
586 Lattice Boltzmann Method (LBM), have successfully been applied in the study of shale
587 gas mechanisms, in particular interests of studying Klinkenberg effect, Knudsen diffu-
588 sion, molecular velocity and many other details of special mechanisms of shale gas flow
589 in reservoirs. Due to the special mechanisms and percolation characteristics of shale
590 gas transport, classical Darcy’s law should be corrected and the concept of apparent

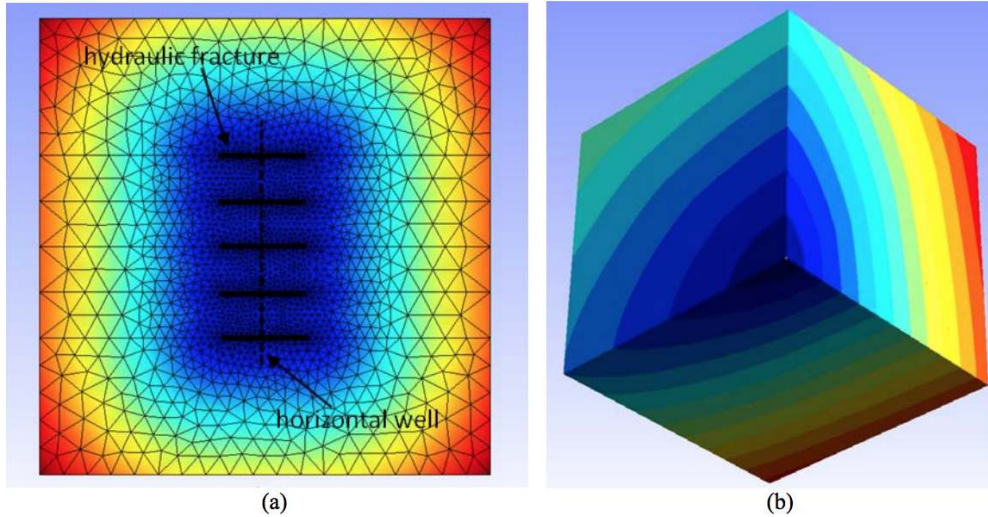


Fig. 7 Fast matching approach simulation examples using unstructured grids (a) 2D examples with isotropic permeability (b) 3D example with anisotropic permeability [186]

591 permeability is introduced. For flow at high rate, e.g. in fractures, improved Darcy's
 592 model with high-order terms of velocity are presented to better describe the gas flow.

593 In reservoir scale flow models, shale is usually classified into four types: inorganic
 594 matter, organic matrix (kerogen), natural fractures, and hydraulic fractures. Various
 595 models of gas transport in shale with detailed description on fracture characterizations
 596 have been developed, including single-porosity, dual porosity and many others. Besides,
 597 it is critical to incorporate general reservoir flow model with geomechanics in order to
 598 better understand the pressure and reservoir performance in hydrocarbon development.
 599 Due to the long history and better visibility, the petroleum industry is more familiar with
 600 macroscopic numerical approaches, including the finite difference method (FDM) and
 601 finite element method (FEM). Recent progress have also been made on other methods,
 602 like finite volume method (FVM) and fast matching method(FMM).

603 Acknowledgements

604 The research reported in this publication was supported in part by funding from King
 605 Abdullah University of Science and Technology (KAUST) through the grant BAS/1/1351-
 606 01-01. The authors are also grateful for financial support from the Beijing Nova Program
 607 under Grant No. Z171100001117081 and the Fundamental Research Funds for the Cen-
 608 tral Universities under Grant No. FRF-TP-17-001C1.

609 References

610 [1] M.-T. Le, "An assessment of the potential for the development
 611 of the shale gas industry in countries outside of north amer-

- 612 ica,” *Heliyon*, vol. 4, no. 2, p. e00516, 2018. [Online]. Available:
613 <http://www.sciencedirect.com/science/article/pii/S2405844017312549>
- 614 [2] Q. Wang, X. Chen, A. N. Jha, and H. Rogers, “Natural gas from shale formation—
615 the evolution, evidences and challenges of shale gas revolution in united states,”
616 *Renewable and Sustainable Energy Reviews*, vol. 30, pp. 1–28
- 617 [3] W. E. Hefley and Y. . . Wang, *Economics of Unconventional Shale Gas Develop-*
618 *ment*. Springer, 2016.
- 619 [4] T. Zhang, A. Salama, S. Sun, and M. F. El-Amin, “Pore network modeling
620 of drainage process in patterned porous media: A quasi-static study,”
621 *Journal of Computational Science*, vol. 9, pp. 64–69, 2015. [Online]. Available:
622 <http://www.sciencedirect.com/science/article/pii/S1877750315000484>
- 623 [5] W. E. Hefley and Y. . . Wang, *Economics of Unconventional Shale Gas Develop-*
624 *ment*. Springer, 2016.
- 625 [6] T. . . Bros, *After the US shale gas revolution*. Editions Technip, 2012.
- 626 [7] Y. Wang and W. E. Hefley, *The Global Impact of Unconventional Shale Gas De-*
627 *velopment: Economics, Policy, and Interdependence*. Springer, 2016, vol. 39
- 628 [8] C. L. Cipolla, E. P. Lolon, J. C. Erdle, and B. Rubin, “Reservoir modeling in
629 shale-gas reservoirs,” 2010.
- 630 [9] B. Rubin, “Accurate simulation of non darcy flow in stimulated fractured shale
631 reservoirs,” 2010.
- 632 [10] X. Wang and T. Wang, *The shale gas potential of China*. Society of Petroleum
633 Engineers, 2011.
- 634 [11] N. C. Reis Jr, J. P. De Angeli, A. F. de Souza, and R. H. Lopes, “Petroleum
635 reservoir simulation using finite volume method with non-structured grids and
636 parallel distributed computing,” 2001.
- 637 [12] R. D. Barree and M. W. Conway, “Beyond beta factors: A complete model for
638 darcy, forchheimer, and trans-forchheimer flow in porous media,” 2004.
- 639 [13] T. Babadagli, S. Raza, X. Ren, and K. Develi, “Effect of sur-
640 face roughness and lithology on the water–gas and water–oil rela-
641 tive permeability ratios of oil-wet single fractures,” *International Jour-*
642 *nal of Multiphase Flow*, vol. 75, pp. 68–81, 2015. [Online]. Available:
643 <http://www.sciencedirect.com/science/article/pii/S0301932215001226>
- 644 [14] R. M. Pollastro, “Total petroleum system assessment of undiscovered resources
645 in the giant barnett shale continuous (unconventional) gas accumulation, fort

- 646 worth basin, texas,” vol. 91, no. 4, pp. 551–578, 2007. [Online]. Available:
647 <http://pubs.er.usgs.gov/publication/70029918>
- 648 [15] X.-C. Lu, F.-C. Li, and A. T. Watson, “Adsorption measurements in devonian
649 shales,” *Fuel*, vol. 74, no. 4, pp. 599–603
- 650 [16] Z. Huan-zhi and H. Yan-qing, *Resource Potential and Development Status of Global
651 Shale Gas [J]*, 2010, vol. 6.
- 652 [17] D. J. K. Ross and R. Marc Bustin, *Shale gas potential of the Lower Jurassic
653 Gordondale Member, Northeastern British Columbia, Canada*, 03 2007, vol. 55.
- 654 [18] J. B. Curtis, “Fractured shale-gas systems,” *AAPG bulletin*, vol. 86, no. 11, pp.
655 1921–1938
- 656 [19] W. V. Grieser, R. F. Shelley, and M. Y. Soliman, *Predicting production outcome
657 from multi-stage, horizontal Barnett completions*. Society of Petroleum Engineers,
658 2009.
- 659 [20] T. Zhang, G. S. Ellis, S. C. Ruppel, K. Milliken, and R. Yang, “Effect of organic-
660 matter type and thermal maturity on methane adsorption in shale-gas systems,”
661 *Organic geochemistry*, vol. 47, pp. 120–131 2012.
- 662 [21] X. Wei, G. Wei, L. Honglin, G. Shusheng, H. Zhiming, and Y. Farong, “Shale reser-
663 voir characteristics and isothermal adsorption properties,” *Natural Gas Industry*,
664 vol. 32, no. 1, pp. 113–116, 2012.
- 665 [22] Z. Zhang and S. Yang, “On the adsorption and desorption trend of shale gas,”
666 *Journal of Experimental Mechanics*, vol. 27, no. 5, pp. 492–497, 2012.
- 667 [23] J. Tan, P. Weniger, B. Krooss, A. Merkel, B. Horsfield, J. Zhang, C. J.
668 Boreham, G. v. Graas, and B. A. Tocher, “Shale gas potential of the major
669 marine shale formations in the upper yangtze platform, south china, part ii:
670 Methane sorption capacity,” *Fuel*, vol. 129, pp. 204–218, 2014. [Online]. Available:
671 <http://www.sciencedirect.com/science/article/pii/S0016236114003159>
- 672 [24] M. G. Bjørner, A. A. Shapiro, and G. M. Kontogeorgis, “Potential theory of
673 adsorption for associating mixtures: possibilities and limitations,” *Industrial En-
674 gineering Chemistry Research*, vol. 52, no. 7, pp. 2672–2684
- 675 [25] T. F. Rexer, M. J. Benham, A. C. Aplin, and K. M. Thomas, “Methane adsorption
676 on shale under simulated geological temperature and pressure conditions,” *Energy
677 Fuels*, vol. 27, no. 6, pp. 3099–3109
- 678 [26] X. Guo, J. Kim, and J. E. Killough, “Hybrid mpi-openmp scalable parallelization
679 for coupled non-isothermal fluid-heat flow and elastoplastic geomechanics,” 2017.

- 680 [27] C. Guo, M. Wei, H. Chen, X. He, and B. Bai, *Improved numerical simulation for*
681 *shale gas reservoirs*. Offshore Technology Conference, 2014.
- 682 [28] H. R. O., “Kapillarchemie, eine darstellung der chemie der kolloide und verwandter
683 gebiete. von dr. herbert freundlich. verlag der akademischen verlagsgesellschaft.
684 leipzig 1909. 591 seiten. preis 16,30 mk., geb. 17,50 mk,” *Zeitschrift für*
685 *Elektrochemie und angewandte physikalische Chemie*, vol. 15, no. 23, pp. 948–948,
686 2018/04/01 2010. [Online]. Available: <https://doi.org/10.1002/bbpc.19090152312>
- 687 [29] I. Langmuir, “The adsorption of gases on plane surfaces of glass, mica and
688 platinum.” *Journal of the American Chemical Society*, vol. 40, no. 9, pp.
689 1361–1403, 09 1918. [Online]. Available: <https://doi.org/10.1021/ja02242a004>
- 690 [30] S. Brunauer, P. H. Emmett, and E. Teller, “Adsorption of gases in multimolecular
691 layers,” *Journal of the American chemical society*, vol. 60, no. 2, pp. 309–319
- 692 [31] M. Dubinin, “The potential theory of adsorption of gases and vapors for adsorbents
693 with energetically nonuniform surfaces.” *Chemical Reviews*, vol. 60, no. 2, pp. 235–
694 241
- 695 [32] —, “Modern state of the theory of gas and vapour adsorption by microporous
696 adsorbents,” *Pure and Applied Chemistry*, vol. 10, no. 4, pp. 309–322
- 697 [33] F. Yang, Z. Ning, and H. Liu, “Fractal characteristics of shales from a shale gas
698 reservoir in the sichuan basin, china,” *Fuel*, vol. 115, pp. 378–384, 2014. [Online].
699 Available: <http://www.sciencedirect.com/science/article/pii/S001623611300639X>
- 700 [34] X. Su, R. Chen, X. Lin, and Y. Song, “Application of adsorption potential theory
701 in the fractionation of coalbed gas during the process of adsorption/desorption,”
702 *Acta Geologica Sinica*, vol. 82, no. 10, pp. 1382–1389, 2008.
- 703 [35] J.-S. Bae and S. K. Bhatia, “High-pressure adsorption of methane and carbon
704 dioxide on coal,” *Energy Fuels*, vol. 20, no. 6, pp. 2599–2607 0887–0624, 2006.
- 705 [36] A. Dada, A. Olalekan, A. Olatunya, and O. Dada, “Langmuir, freundlich, temkin
706 and dubinin–radushkevich isotherms studies of equilibrium sorption of zn²⁺ unto
707 phosphoric acid modified rice husk,” *IOSR Journal of Applied Chemistry*, vol. 3,
708 no. 1, pp. 38–45, 2012.
- 709 [37] T. Zhang, G. S. Ellis, S. C. Ruppel, K. Milliken, and R. Yang, “Effect of
710 organic-matter type and thermal maturity on methane adsorption in shale-gas
711 systems,” *Organic Geochemistry*, vol. 47, pp. 120–131, 2012. [Online]. Available:
712 <http://www.sciencedirect.com/science/article/pii/S0146638012000629>
- 713 [38] M. A. Ahmadi and S. R. Shadizadeh, “Experimental investigation of a
714 natural surfactant adsorption on shale-sandstone reservoir rocks: Static and

- 715 dynamic conditions,” *Fuel*, vol. 159, pp. 15–26, 2015. [Online]. Available:
716 <http://www.sciencedirect.com/science/article/pii/S0016236115006158>
- 717 [39] L. Ming, G. Anzhong, L. Xuesheng, and W. Rongshun, “Determination of the
718 adsorbate density from supercritical gas adsorption equilibrium data,” *Carbon*,
719 vol. 3, no. 41, pp. 585–588
- 720 [40] S. Chen, Y. Zhu, H. Wang, H. Liu, W. Wei, and J. Fang, “Shale gas
721 reservoir characterisation: A typical case in the southern sichuan basin of
722 china,” *Energy*, vol. 36, no. 11, pp. 6609–6616, 2011. [Online]. Available:
723 <http://www.sciencedirect.com/science/article/pii/S0360544211005986>
- 724 [41] X. Luo, S. Wang, Z. Wang, Z. Jing, M. Lv, Z. Zhai, and T. Han, “Adsorption
725 of methane, carbon dioxide and their binary mixtures on jurassic shale from the
726 qaidam basin in china,” *International Journal of Coal Geology*, vol. 150, pp. 210–
727 223
- 728 [42] W. Yu, K. Sepehrnoori, and T. W. Patzek, “Modeling gas adsorption in marcellus
729 shale with langmuir and bet isotherms,” 2016.
- 730 [43] T. F. T. Rexer, M. J. Benham, A. C. Aplin, and K. M. Thomas, “Methane
731 adsorption on shale under simulated geological temperature and pressure
732 conditions,” *Energy & Fuels*, vol. 27, no. 6, pp. 3099–3109, 06 2013. [Online].
733 Available: <https://doi.org/10.1021/ef400381v>
- 734 [44] X. Tang, N. Ripepi, N. P. Stadie, L. Yu, and M. R. Hall, “A
735 dual-site langmuir equation for accurate estimation of high pressure deep
736 shale gas resources,” *Fuel*, vol. 185, pp. 10–17, 2016. [Online]. Available:
737 <http://www.sciencedirect.com/science/article/pii/S0016236116306913>
- 738 [45] F. O. Mertens, “Determination of absolute adsorption in highly ordered porous
739 media,” *Surface Science*, vol. 603, no. 10-12, pp. 1979–1984 0039–6028, 2009.
- 740 [46] X. Tang and N. Ripepi, “High pressure supercritical carbon dioxide adsorption
741 in coal: Adsorption model and thermodynamic characteristics,” *Journal of CO2
742 Utilization*, vol. 18, pp. 189–197
- 743 [47] N. P. Stadie, M. Murialdo, C. C. Ahn, and B. Fultz, “Unusual entropy of adsorbed
744 methane on zeolite-templated carbon,” *The Journal of Physical Chemistry C*, vol.
745 119, no. 47, pp. 26 409–26 421
- 746 [48] J. Saulsberry, P. Schafer, R. Schraufnagel, and G. R. I. (U.S.), *A Guide to
747 Coalbed Methane Reservoir Engineering*. Gas Research Institute, 1996. [Online].
748 Available: <https://books.google.com.sa/books?id=D4UuuAAACAAJ>

- 749 [49] G. H. Z. X. C. L. L. D. L. J. Shen, Y., “Impact of fracturing liquid absorption
750 on the production and water-block unlocking for shale gas reservoir,” *Advances in*
751 *Geo-Energy Research*, vol. 2, no. 2, pp. 163–172, 2018.
- 752 [50] Y. Zhou and L. Zhou, “Fundamentals of high pressure adsorption,” *Langmuir*,
753 vol. 25, no. 23, pp. 13 461–13 466
- 754 [51] M. Dubinin, “The potential theory of adsorption of gases and vapors for adsorbents
755 with energetically nonuniform surfaces.” *Chemical Reviews*, vol. 60, no. 2, pp. 235–
756 241
- 757 [52] R. J. Ambrose, R. C. Hartman, and I. Y. Akkutlu, “Multi-component sorbed
758 phase considerations for shale gas-in-place calculations,” p. 10, 2011. [Online].
759 Available: <https://doi.org/10.2118/141416-MS>
- 760 [53] R. C. Hartman, R. J. Ambrose, I. Y. Akkutlu, and C. R. Clarkson, “Shale
761 gas-in-place calculations part ii - multicomponent gas adsorption effects,” p. 17,
762 2011. [Online]. Available: <https://doi.org/10.2118/144097-MS>
- 763 [54] E. Fathi and I. Y. Akkutlu, “Multi-component gas transport and adsorption
764 effects during co2 injection and enhanced shale gas recovery,” *International*
765 *Journal of Coal Geology*, vol. 123, pp. 52–61, 2014. [Online]. Available:
766 <http://www.sciencedirect.com/science/article/pii/S0166516213001808>
- 767 [55] J. Jiang, Y. Shao, and R. M. Younis, “Development of a multi-continuum multi-
768 component model for enhanced gas recovery and co2 storage in fractured shale gas
769 reservoirs,” p. 17, 2014. [Online]. Available: <https://doi.org/10.2118/169114-MS>
- 770 [56] K. M. Gerke, M. V. Karsanina, and D. Mallants, “Universal stochastic multiscale
771 image fusion: an example application for shale rock,” *Scientific reports*, vol. 5, pp.
772 15 880
- 773 [57] J. Di and J. Jensen, “A closer look at pore throat size estimators for tight gas
774 formations,” *Journal of Natural Gas Science and Engineering*, vol. 27, pp. 1252–
775 1260
- 776 [58] W. D. . . McCain, *The properties of petroleum fluids*. PennWell Books, 1990.
- 777 [59] J. Kärger, “Flow and transport in porous media and fractured rock,” *Zeitschrift*
778 *für Physikalische Chemie*, vol. 194, no. 1, pp. 135–136
- 779 [60] J. Zhao, L. Yang, K. Xue, W. Lam, Y. Li, and Y. Song, “In situ observation of
780 gas hydrates growth hosted in porous media,” *Chemical Physics Letters*, vol. 612,
781 pp. 124–128
- 782 [61] W. He, J. Zou, B. Wang, S. Vilayurganapathy, M. Zhou, X. Lin, K. H. Zhang,
783 J. Lin, P. Xu, and J. H. Dickerson, “Gas transport in porous electrodes of solid

- 784 oxide fuel cells: a review on diffusion and diffusivity measurement,” *Journal of*
785 *Power Sources*, vol. 237, pp. 64–73
- [62] B. Berkowitz and R. P. Ewing, “Percolation theory and network modeling appli-
786 cations in soil physics,” *Surveys in Geophysics*, vol. 19, no. 1, pp. 23–72
787
- [63] A. Beskok, G. E. Karniadakis, and W. Trimmer, “Rarefaction and compressibility
788 effects in gas microflows,” *Journal of Fluids Engineering*, vol. 118, no. 3, pp.
789 448–456, 09 1996. [Online]. Available: <http://dx.doi.org/10.1115/1.2817779>
790
- [64] E. Ozkan, R. S. Raghavan, and O. G. Apaydin, “Modeling of fluid transfer from
791 shale matrix to fracture network,” 2010.
792
- [65] H. ZHAO, M. CHEN, Y. JIN, Y. DING, and Y. WANG, “Rock fracture kinetics
793 of the fracture mesh system in shale gas reservoirs,” *Petroleum Exploration*
794 *and Development*, vol. 39, no. 4, pp. 498–503, 2012. [Online]. Available:
795 <http://www.sciencedirect.com/science/article/pii/S1876380412600676>
796
- [66] H. Song, Y. Wang, J. Wang, and Z. Li, “Unifying diffusion and
797 seepage for nonlinear gas transport in multiscale porous media,” *Chem-*
798 *ical Physics Letters*, vol. 661, pp. 246–250, 2016. [Online]. Available:
799 <http://www.sciencedirect.com/science/article/pii/S0009261416304687>
800
- [67] C. Tian, Y. Chao, Y. Ying, D. Yan-Hong, G. Shui-Bin, X. Yi-Jun, N. Zhao-Yuan,
801 P. Xiao-Ping, and W. Zhen-Ming, “Photoluminescence of silicone oil treated
802 by fluorocarbon plasma,” *Chinese Physics B*, vol. 21, no. 9, p. 097802, 2012.
803 [Online]. Available: <http://stacks.iop.org/1674-1056/21/i=9/a=097802>
804
- [68] C. Neto, D. R. Evans, E. Bonaccorso, H.-J. Butt, and V. S. Craig, “Boundary slip
805 in newtonian liquids: a review of experimental studies,” *Reports on Progress in*
806 *Physics*, vol. 68, no. 12, pp. 2859
807
- [69] M. T. Matthews and J. M. Hill, “Nanofluidics and the navier boundary condition,”
808 *International Journal of Nanotechnology*, vol. 5, no. 2-3, pp. 218–242
809
- [70] Z. Li, C. Wei, J. Leung, Y. Wang, and H. Song, “Numerical and experimental
810 study on gas flow in nanoporous media,” *Journal of Natural Gas Science and*
811 *Engineering*, vol. 27, pp. 738–744
812
- [71] S. Whitaker, “Flow in porous media i: A theoretical derivation of darcy’s law,”
813 *Transport in porous media*, vol. 1, no. 1, pp. 3–25 0169–3913, 1986.
814
- [72] A. S. Ziarani and R. Aguilera, “Knudsen’s permeability correction for tight porous
815 media,” *Transport in porous media*, vol. 91, no. 1, pp. 239–260
816
- [73] X.-D. Shan and M. Wang, “Effective resistance of gas flow in microchannels,”
817 *Advances in Mechanical Engineering*, vol. 5, pp. 950 681 1687–8140, 2013.
818

- 819 [74] H. Song, Y. Wang, J. Wang, and Z. Li, “Unifying diffusion and seepage for non-
820 linear gas transport in multiscale porous media,” *Chemical Physics Letters*, vol.
821 661, pp. 246–250
- 822 [75] T. G. Myers, “Why are slip lengths so large in carbon nanotubes?” *Microfluidics
823 and Nanofluidics*, vol. 10, no. 5, pp. 1141–1145, 2011. [Online]. Available:
824 <https://doi.org/10.1007/s10404-010-0752-7>
- 825 [76] P.-G. de Gennes, “On fluid/wall slippage,” *Langmuir*, vol. 18, no. 9, pp. 3413–3414
- 826 [77] J. C. T. Eijkel and A. v. d. Berg, “Nanofluidics: what is it and what can we
827 expect from it?” *Microfluidics and Nanofluidics*, vol. 1, no. 3, pp. 249–267, 2005.
828 [Online]. Available: <https://doi.org/10.1007/s10404-004-0012-9>
- 829 [78] R. J. Ambrose, R. C. Hartman, M. Diaz Campos, I. Y. Akkutlu, and C. Sondergeld,
830 “New pore-scale considerations for shale gas in place calculations,” 2010.
- 831 [79] W. Wei and Y. Xia, “Geometrical, fractal and hydraulic properties of fractured
832 reservoirs: A mini-review,” *Adv. Geo Energy*, vol. 1, no. 1, pp. 31–38, 2017.
- 833 [80] Z. Tan, W. Wang, W. Li, S. Lu, and T. He, “Controlling factors and physical
834 property cutoffs of the tight reservoir in the liuhe basin,” *ADVANCES IN GEO-
835 ENERGY RESEARCH*, vol. 1, pp. 190–202, 12 2017.
- 836 [81] S. Yinghao, H. Ge, X. Zhang, L. Chang, L. Dunqing, and J. Liu, “Impact of
837 fracturing liquid absorption on the production and water-block unlocking for shale
838 gas reservoir,” *ADVANCES IN GEO-ENERGY RESEARCH*, vol. 2, pp. 163–172,
839 06 2018.
- 840 [82] J. Cai, W. Wei, X. Hu, R. Liu, and J. Wang, “Fractal characterization of dynamic
841 fracture network extension in porous media,” *Fractals*, vol. 25, no. 02, pp. 1 750 023
- 842 [83] N. G. Hadjiconstantinou, “The limits of navier-stokes theory and kinetic exten-
843 sions for describing small-scale gaseous hydrodynamics,” *Physics of Fluids*, vol. 18,
844 no. 11, pp. 111 301
- 845 [84] C. V. . . Heer, *Statistical mechanics, kinetic theory, and stochastic processes*. El-
846 sevier, 2012.
- 847 [85] G. Bird, “Molecular gas dynamics and the direct simulation monte carlo of gas
848 flows,” *Clarendon, Oxford*, vol. 508, p. 128, 1994.
- 849 [86] J. Koplik and J. R. Banavar, “Continuum deductions from molecular hydrody-
850 namics,” *Annual Review of Fluid Mechanics*, vol. 27, no. 1, pp. 257–292
- 851 [87] A. Sharma, S. Namsani, and J. K. Singh, “Molecular simulation of shale gas
852 adsorption and diffusion in inorganic nanopores,” *Molecular Simulation*, vol. 41,
853 no. 5-6, pp. 414–422

- 854 [88] Z. Jin and A. Firoozabadi, “Flow of methane in shale nanopores at low and
855 high pressure by molecular dynamics simulations,” *The Journal of Chemical*
856 *Physics*, vol. 143, no. 10, p. 104315, 2018/04/04 2015. [Online]. Available:
857 <https://doi.org/10.1063/1.4930006>
- 858 [89] H. Wu, J. Chen, and H. Liu, “Molecular dynamics simulations about adsorption
859 and displacement of methane in carbon nanochannels,” *The Journal of Physical*
860 *Chemistry C*, vol. 119, no. 24, pp. 13 652–13 657 2015.
- 861 [90] J. A. Thomas and A. J. H. McGaughey, “Water flow in carbon nan-
862 otubes: Transition to subcontinuum transport,” *Physical Review Let-*
863 *ters*, vol. 102, no. 18, pp. 184502–, 05 2009. [Online]. Available:
864 <https://link.aps.org/doi/10.1103/PhysRevLett.102.184502>
- 865 [91] X. Yang and C. Zhang, *Structure and diffusion behavior of dense carbon dioxide*
866 *fluid in clay-like slit pores by molecular dynamics simulation*, 05 2005, vol. 407.
- 867 [92] A. Botan, B. Rotenberg, V. Marry, P. Turq, and B. Noetinger, “Carbon dioxide
868 in montmorillonite clay hydrates: thermodynamics, structure, and transport from
869 molecular simulation,” *The Journal of Physical Chemistry C*, vol. 114, no. 35, pp.
870 14 962–14 969
- 871 [93] R. T. Cygan, V. N. Romanov, and E. M. Myshakin, “Molecular simulation of
872 carbon dioxide capture by montmorillonite using an accurate and flexible force
873 field,” *The Journal of Physical Chemistry C*, vol. 116, no. 24, pp. 13 079–13 091
- 874 [94] M. Firouzi, E. C. Rupp, C. W. Liu, and J. Wilcox, “Molecular simulation and
875 experimental characterization of the nanoporous structures of coal and gas shale,”
876 *International Journal of Coal Geology*, vol. 121, pp. 123–128, 2014. [Online].
877 Available: <http://www.sciencedirect.com/science/article/pii/S0166516213002498>
- 878 [95] Q. Yuan, X. Zhu, K. Lin, and Y.-P. Zhao, “Molecular dynamics simulations of the
879 enhanced recovery of confined methane with carbon dioxide,” *Physical Chemistry*
880 *Chemical Physics*, vol. 17, no. 47, pp. 31 887–31 893, 2015.
- 881 [96] X. Zhang, L. Xiao, X. Shan, and L. Guo, “Lattice boltzmann simulation of shale
882 gas transport in organic nano-pores,” *Scientific reports*, vol. 4, pp. 4843
- 883 [97] L. Chen, L. Zhang, Q. Kang, H. S. Viswanathan, J. Yao, and W. Tao, “Nanoscale
884 simulation of shale transport properties using the lattice boltzmann method: per-
885 meability and diffusivity,” *Scientific reports*, vol. 5, pp. 8089
- 886 [98] H. Huang and X.-y. Lu, “Relative permeabilities and coupling effects in
887 steady-state gas-liquid flow in porous media: A lattice boltzmann study,” *Physics*
888 *of Fluids*, vol. 21, no. 9, p. 092104, 2018/03/20 2009. [Online]. Available:
889 <https://doi.org/10.1063/1.3225144>

- 890 [99] E. Fathi and I. Y. Akkutlu, “Lattice boltzmann method for simulation of shale
891 gas transport in kerogen,” 2012.
- 892 [100] E. Fathi, A. Tinni, and I. Y. Akkutlu, *Shale gas correction to Klinkenberg slip*
893 *theory*. Society of Petroleum Engineers, 2012.
- 894 [101] H. Song, M. Yu, W. Zhu, P. Wu, Y. Lou, Y. Wang, and J. Killough, “Numerical
895 investigation of gas flow rate in shale gas reservoirs with nanoporous media,” *Inter-*
896 *national Journal of Heat and Mass Transfer*, vol. 80, pp. 626–635, 2015. [Online].
897 Available: <http://www.sciencedirect.com/science/article/pii/S001793101400831X>
- 898 [102] J. Ma, J. P. Sanchez, K. Wu, G. D. Couples, and Z. Jiang, “A pore
899 network model for simulating non-ideal gas flow in micro- and nano-
900 porous materials,” *Fuel*, vol. 116, pp. 498–508, 2014. [Online]. Available:
901 <http://www.sciencedirect.com/science/article/pii/S0016236113007692>
- 902 [103] T. Cao, Z. Song, S. Wang, X. Cao, Y. Li, and J. Xia, “Characterizing the
903 pore structure in the silurian and permian shales of the sichuan basin, china,”
904 *Marine and Petroleum Geology*, vol. 61, pp. 140–150, 2015. [Online]. Available:
905 <http://www.sciencedirect.com/science/article/pii/S0264817214003754>
- 906 [104] X. Huang, K. W. Bandilla, and M. A. Celia, “Multi-physics pore-network modeling
907 of two-phase shale matrix flows,” *Transport in Porous Media*, vol. 111, no. 1, pp.
908 123–141, 2016. [Online]. Available: <https://doi.org/10.1007/s11242-015-0584-8>
- 909 [105] K. Wua, X. Li, C. Guo, and Z. Chen, “Adsorbed gas surface diffusion and bulk
910 gas transport in nanopores of shale reservoirs with real gas effect-adsorption-
911 mechanical coupling,” 2015.
- 912 [106] H. Darcy, “Les fontaines publiques de la ville de dijon (dalmont, paris, 1856),”
913 *Google Scholar*, pp. 305–401, 2007.
- 914 [107] T. V. Nguyen, “Experimental study of non-darcy flow through perforations,” 1986.
- 915 [108] L. Klinkenberg, *The permeability of porous media to liquids and gases*. American
916 Petroleum Institute, 1941.
- 917 [109] F. O. Jones and W. Owens, “A laboratory study of low-permeability gas sands,”
918 *Journal of Petroleum Technology*, vol. 32, no. 09, pp. 1,631–1,640 0149–2136, 1980.
- 919 [110] K. Sampath and C. W. Keighin, “Factors affecting gas slippage in tight sandstones
920 of cretaceous age in the uinta basin,” *Journal of Petroleum Technology*, vol. 34,
921 no. 11, pp. 2,715–2,720
- 922 [111] F. Civan, “Effective correlation of apparent gas permeability in tight porous me-
923 dia,” *Transport in porous media*, vol. 82, no. 2, pp. 375–384 0169–3913, 2010.

- 924 [112] A. Beskok and G. E. Karniadakis, “Report: a model for flows in channels, pipes,
925 and ducts at micro and nano scales,” *Microscale Thermophysical Engineering*,
926 vol. 3, no. 1, pp. 43–77
- 927 [113] A. Sakhaee-Pour and S. Bryant, “Gas permeability of shale,” 2012.
- 928 [114] W. Pollard and R. D. Present, “On gaseous self-diffusion in long capillary tubes,”
929 *Physical Review*, vol. 73, no. 7, p. 762, 1948.
- 930 [115] H. Sun, A. Chawathe, H. Hoteit, X. Shi, and L. Li, “Understanding shale gas flow
931 behavior using numerical simulation,” *SPE Journal*, vol. 20, no. 01, pp. 142–154
- 932 [116] Y. He, J. Cheng, X. Dou, and X. Wang, “Research on shale gas
933 transportation and apparent permeability in nanopores,” *Journal of Natural
934 Gas Science and Engineering*, vol. 38, pp. 450–457, 2017. [Online]. Available:
935 <http://www.sciencedirect.com/science/article/pii/S1875510016309325>
- 936 [117] B. Ghanbarian and F. Javadpour, “Upscaling pore pressure-dependent
937 gas permeability in shales,” *Journal of Geophysical Research: Solid
938 Earth*, vol. 122, no. 4, pp. 2541–2552, 2017. [Online]. Available:
939 <https://agupubs.onlinelibrary.wiley.com/doi/abs/10.1002/2016JB013846>
- 940 [118] D. Li and T. W. Engler, “Literature review on correlations of the non-darcy coef-
941 ficient,” 2001.
- 942 [119] H. Belhaj, K. Agha, A. Nouri, S. Butt, and M. Islam, *Numerical and experimental
943 modeling of non-Darcy flow in porous media*. Society of Petroleum Engineers,
944 2003.
- 945 [120] D. Takhanov, “Forchheimer model for non-darcy flow in porous media and frac-
946 tures,” 2011.
- 947 [121] A. . . Bejan, *Convection heat transfer*. John wiley sons, 2013.
- 948 [122] B. Lai, J. L. Miskimins, and Y.-S. Wu, “Non-darcy porous-media flow according
949 to the barree and conway model: Laboratory and numerical-modeling studies,”
950 2012.
- 951 [123] A. Al-Otaibi and Y.-S. Wu, *An alternative approach to modeling non-Darcy flow
952 for pressure transient analysis in porous and fractured reservoirs*. Society of
953 Petroleum Engineers, 2011.
- 954 [124] Y.-S. Wu, B. Lai, J. L. Miskimins, P. Fakcharoenphol, and Y. Di, “Analysis of
955 multiphase non-darcy flow in porous media,” *Transport in Porous Media*, vol. 88,
956 no. 2, pp. 205–223, 2011. [Online]. Available: [https://doi.org/10.1007/s11242-
957 011-9735-8](https://doi.org/10.1007/s11242-011-9735-8)

- 958 [125] R. D. Barree and M. Conway, “Multiphase non-darcy flow in proppant packs,”
959 2007.
- 960 [126] B. Lai, J. L. Miskimins, and Y.-S. Wu, “Non-darcy porous-media flow according
961 to the barree and conway model: Laboratory and numerical-modeling studies,”
962 2012.
- 963 [127] F. Javadpour, “Nanopores and apparent permeability of gas flow in mudrocks
964 (shales and siltstone),” *Journal of Canadian Petroleum Technology*, vol. 48, no. 08,
965 pp. 16–21
- 966 [128] R. G. Loucks, R. M. Reed, S. C. Ruppel, and U. Hammes, “Spectrum of pore
967 types and networks in mudrocks and a descriptive classification for matrix-related
968 mudrock pores,” *AAPG bulletin*, vol. 96, no. 6, pp. 1071–1098 0149–1423, 2012.
- 969 [129] M. E. Curtis, R. J. Ambrose, and C. H. Sondergeld, *Structural characterization of*
970 *gas shales on the micro-and nano-scales*. Society of Petroleum Engineers, 2010.
- 971 [130] D. Jarvie, R. Pollastro, R. Hill, K. Bowker, B. Claxton, and J. Burgess, *Evaluation*
972 *of hydrocarbon generation and storage in the Barnett Shale, Ft. Worth Basin,*
973 *Texas*, 2004.
- 974 [131] I. D. Sulucarnain, C. H. Sondergeld, and C. S. Rai, *An NMR study of shale wet-*
975 *tability and effective surface relaxivity*. Society of Petroleum Engineers, 2012.
- 976 [132] F. P. Wang and R. M. Reed, *Pore networks and fluid flow in gas shales*. Society
977 of Petroleum Engineers, 2009.
- 978 [133] J. D. Hudson, F. Civan, G. Michel, D. Devegowda, and R. F. Sigal, *Modeling*
979 *multiple-porosity transport in gas-bearing shale formations*. Society of Petroleum
980 Engineers, 2012.
- 981 [134] B. Yan, Y. Wang, and J. E. Killough, “Beyond dual-porosity modeling
982 for the simulation of complex flow mechanisms in shale reservoirs,” *Com-*
983 *putational Geosciences*, vol. 20, no. 1, pp. 69–91, 2016. [Online]. Available:
984 <https://doi.org/10.1007/s10596-015-9548-x>
- 985 [135] Y.-S. Wu, G. J. Moridis, B. Bai, and K. Zhang, “A multi-continuum model for
986 gas production in tight fractured reservoirs,” 2009.
- 987 [136] D. Y. Ding, H. Langouët, and L. Jeannin, “Simulation of fracturing-induced for-
988 mation damage and gas production from fractured wells in tight gas reservoirs,”
989 *SPE Production Operations*, vol. 28, no. 03, pp. 246–258
- 990 [137] D. Y. Ding, Y. Wu, and L. Jeannin, “Efficient simulation of hydraulic fractured
991 wells in unconventional reservoirs,” *Journal of Petroleum Science and Engineering*,
992 vol. 122, pp. 631–642

- 993 [138] C. Clarkson and T. Ertekin, *A new model for shale gas matrix flow using the*
994 *dynamic-slippage concept*, 2010.
- 995 [139] M. E. Curtis, C. H. Sondergeld, R. J. Ambrose, and C. S. Rai, “Microstructural
996 investigation of gas shales in two and three dimensions using nanometer-scale
997 resolution imagingmicrostructure of gas shales,” *AAPG bulletin*, vol. 96, no. 4,
998 pp. 665–677
- 999 [140] A. S. Ziarani and R. Aguilera, “Knudsen’s permeability correction for tight porous
1000 media,” *Transport in porous media*, vol. 91, no. 1, pp. 239–260
- 1001 [141] C. Guo, M. Wei, and H. Liu, “Study of gas production from shale reservoirs with
1002 multi-stage hydraulic fracturing horizontal well considering multiple transport
1003 mechanisms,” *PLoS ONE*, vol. 13, no. 1, p. e0188480, 2018. [Online]. Available:
1004 <http://www.ncbi.nlm.nih.gov/pmc/articles/PMC5761844/>
- 1005 [142] R. H. Dean, X. Gai, C. M. Stone, and S. E. Minkoff, “A comparison of techniques
1006 for coupling porous flow and geomechanics,” 2006.
- 1007 [143] W. M. F. and G. Xiuli, “Iteratively coupled mixed and galerkin finite
1008 element methods for poro-elasticity,” *Numerical Methods for Partial Differential*
1009 *Equations*, vol. 23, no. 4, pp. 785–797, 2018/03/18 2007. [Online]. Available:
1010 <https://doi.org/10.1002/num.20258>
- 1011 [144] F. O. Alpak, “Robust fully-implicit coupled multiphase-flow and geomechanics
1012 simulation,” 2015.
- 1013 [145] J. Cai and B. Yu, “A discussion of the effect of tortuosity on the capillary
1014 imbibition in porous media,” *Transport in Porous Media*, vol. 89, no. 2, pp.
1015 251–263, 2011. [Online]. Available: <https://doi.org/10.1007/s11242-011-9767-0>
- 1016 [146] J. Cai, B. Yu, M. Zou, and L. Luo, “Fractal characterization of spontaneous
1017 co-current imbibition in porous media,” *Energy & Fuels*, vol. 24, no. 3, pp.
1018 1860–1867, 03 2010. [Online]. Available: <https://doi.org/10.1021/ef901413p>
- 1019 [147] W. Guo, Z. Hu, X. Zhang, R. Yu, and L. Wang, “Shale gas adsorption
1020 and desorption characteristics and its effects on shale permeability,” *Energy*
1021 *Exploration & Exploitation*, vol. 35, no. 4, pp. 463–481, 2018/03/25 2017.
1022 [Online]. Available: <https://doi.org/10.1177/0144598716684306>
- 1023 [148] S. E. Minkoff, C. M. Stone, S. Bryant, M. Peszynska, and M. F. Wheeler,
1024 “Coupled fluid flow and geomechanical deformation modeling,” *Journal of*
1025 *Petroleum Science and Engineering*, vol. 38, no. 1, pp. 37–56, 2003. [Online].
1026 Available: <http://www.sciencedirect.com/science/article/pii/S0920410503000214>
- 1027 [149] X. Guo, H. Song, K. Wu, and J. Killough, “Pressure characteristics
1028 and performance of multi-stage fractured horizontal well in shale gas

- 1029 reservoirs with coupled flow and geomechanics,” *Journal of Petroleum*
1030 *Science and Engineering*, vol. 163, pp. 1–15, 2018. [Online]. Available:
1031 <http://www.sciencedirect.com/science/article/pii/S0920410517309956>
- 1032 [150] J. Gupta, M. Zielonka, R. A. Albert, A. M. El-Rabaa, H. A. Burnham, and N. H.
1033 Choi, “Integrated methodology for optimizing development of unconventional gas
1034 resources,” 2012.
- 1035 [151] W. Yu, Z. Luo, F. Javadpour, A. Varavei, and K. Sepehrnoori, “Sensitivity
1036 analysis of hydraulic fracture geometry in shale gas reservoirs,” *Journal of*
1037 *Petroleum Science and Engineering*, vol. 113, pp. 1–7, 2014. [Online]. Available:
1038 <http://www.sciencedirect.com/science/article/pii/S0920410513003537>
- 1039 [152] M. Moradi, F. Imani, H. Naji, S. Moradi Behbahani, and M. Taghi Ahmadi, *Vari-*
1040 *ation in soil carbon stock and nutrient content in sand dunes after afforestation*
1041 *by Prosopis juliflora in the Khuzestan province (Iran)*, 05 2017, vol. 10.
- 1042 [153] C. An, Y. Fang, S. Liu, M. Alfi, B. Yan, Y. Wang, and J. Killough, *Impacts*
1043 *of Matrix Shrinkage and Stress Changes on Permeability and Gas Production of*
1044 *Organic-Rich Shale Reservoirs*, 05 2017.
- 1045 [154] I. Shovkun and D. N. Espinoza, “Coupled fluid flow-geomechanics simulation in
1046 stress-sensitive coal and shale reservoirs: Impact of desorption-induced stresses,
1047 shear failure, and fines migration,” *Fuel*, vol. 195, pp. 260–272, 2017. [Online].
1048 Available: <http://www.sciencedirect.com/science/article/pii/S0016236117300650>
- 1049 [155] C. Wei, L. Wang, B. Li, L. Xiong, S. Liu, J. Zheng, S. Hu, and H. Song, *A Study*
1050 *of Nonlinear Elasticity Effects on Permeability of Stress Sensitive Shale Rocks*
1051 *Using an Improved Coupled Flow and Geomechanics Model: A Case Study of the*
1052 *Longmaxi Shale in China*, 02 2018, vol. 11.
- 1053 [156] V. Shabro, C. Torres-Verdín, F. Javadpour, and K. Sepehrnoori, “Finite-difference
1054 approximation for fluid-flow simulation and calculation of permeability in porous
1055 media,” *Transport in porous media*, vol. 94, no. 3, pp. 775–793
- 1056 [157] E. Nacul, C. Lepretre, O. Pedrosa Jr, P. Girard, and K. Aziz, *Efficient use of*
1057 *domain decomposition and local grid refinement in reservoir simulation*. Society
1058 of Petroleum Engineers, 1990.
- 1059 [158] T. Ertekin, J. H. Abou-Kassen, and G. R. . . King, *Basic applied reservoir simu-*
1060 *lations*. Society of Petroleum Engineers, 2001.
- 1061 [159] A. . . Firoozabadi, *Thermodynamics of hydrocarbon reservoirs*. McGraw-Hill,
1062 1999.

- 1063 [160] R. Jayakumar, V. Sahai, and A. Boulis, *A better understanding of finite element*
1064 *simulation for shale gas reservoirs through a series of different case histories.*
1065 Society of Petroleum Engineers, 2011.
- 1066 [161] R. Logan, R. Lee, and M. Tek, *Microcomputer gas reservoir simulation using finite*
1067 *element methods.* Society of Petroleum Engineers, 1985.
- 1068 [162] G. J. Moridis, T. A. Blasingame, and C. M. Freeman, *Analysis of mechanisms of*
1069 *flow in fractured tight-gas and shale-gas reservoirs.* Society of Petroleum Engi-
1070 neers, 2010.
- 1071 [163] K. Aziz and A. . . Settari, *Petroleum reservoir simulation.* Chapman Hall, 1979.
- 1072 [164] Z. Heinemann, C. Brand, M. Munka, and Y. Chen, *Modeling reservoir geometry*
1073 *with irregular grids.* Society of Petroleum Engineers, 1989.
- 1074 [165] L. Zhang, D. Li, L. Wang, and D. Lu, “Simulation of gas transport in tight/shale
1075 gas reservoirs by a multicomponent model based on pebi grid,” *Journal of Chem-*
1076 *istry*, vol. 2015
- 1077 [166] J. Sun, D. Schechter, and C.-K. Huang, “Grid-sensitivity analysis and compari-
1078 son between unstructured perpendicular bisector and structured tartan/local-grid-
1079 refinement grids for hydraulically fractured horizontal wells in eagle ford formation
1080 with complicated natural fractures,” 2016.
- 1081 [167] Y. Yang, S. Fu, and E. T. Chung, “Online mixed multiscale finite element method
1082 with oversampling and its applications,” *arXiv preprint arXiv:1807.00710*, 2018.
- 1083 [168] E. T. Chung, Y. Efendiev, and W. T. Leung, “Residual-driven online generalized
1084 multiscale finite element methods,” *Journal of Computational Physics*, vol. 302,
1085 pp. 176–190
- 1086 [169] M. Alotaibi, V. M. Calo, Y. Efendiev, J. Galvis, and M. Ghommem, “Global–local
1087 nonlinear model reduction for flows in heterogeneous porous media,” *Computer*
1088 *Methods in Applied Mechanics and Engineering*, vol. 292, pp. 122–137
- 1089 [170] X. Chen, G. Yao, J. Cai, Y. Huang, and X. Yuan, “Fractal and multifractal analysis
1090 of different hydraulic flow units based on micro-ct images,” *Journal of Natural Gas*
1091 *Science and Engineering*, vol. 48, pp. 145–156
- 1092 [171] Y. Efendiev and T. Y. Hou, *Multiscale finite element methods: theory and appli-*
1093 *cations.* Springer Science Business Media, 2009, vol. 4
- 1094 [172] I. Babuška, G. Caloz, and J. E. Osborn, “Special finite element methods for a
1095 class of second order elliptic problems with rough coefficients,” *SIAM Journal on*
1096 *Numerical Analysis*, vol. 31, no. 4, pp. 945–981 0036–1429, 1994.

- 1097 [173] T. Arbogast, “Implementation of a locally conservative numerical subgrid upscal-
1098 ing scheme for two-phase darcy flow,” *Computational Geosciences*, vol. 6, no. 3-4,
1099 pp. 453–481
- 1100 [174] Z. Chen and T. Hou, “A mixed multiscale finite element method for elliptic prob-
1101 lems with oscillating coefficients,” *Mathematics of Computation*, vol. 72, no. 242,
1102 pp. 541–576
- 1103 [175] T. Arbogast, G. Pencheva, M. F. Wheeler, and I. Yotov, “A multiscale mortar
1104 mixed finite element method,” *Multiscale Modeling Simulation*, vol. 6, no. 1, pp.
1105 319–346
- 1106 [176] O. Møyner and K.-A. Lie, “A multiscale restriction-smoothed basis method
1107 for high contrast porous media represented on unstructured grids,” *Journal*
1108 *of Computational Physics*, vol. 304, pp. 46–71, 2016. [Online]. Available:
1109 <http://www.sciencedirect.com/science/article/pii/S0021999115006725>
- 1110 [177] P. Vanek, J. Mandel, and M. Brezina, “Algebraic multigrid on unstructured
1111 meshes,” *University of Colorado at Denver, UCD= CCM Report*, no. 34, 1994.
- 1112 [178] P. Vaněk, J. Mandel, and M. Brezina, “Algebraic multigrid by smoothed aggrega-
1113 tion for second and fourth order elliptic problems,” *Computing*, vol. 56, no. 3, pp.
1114 179–196
- 1115 [179] M. Brezina, R. Falgout, S. MacLachlan, T. Manteuffel, S. McCormick, and J. Ruge,
1116 “Adaptive smoothed aggregation (sa) multigrid,” *SIAM review*, vol. 47, no. 2, pp.
1117 317–346
- 1118 [180] K. Stüben, *A review of algebraic multigrid*. Elsevier, 2001, pp. 281–309.
- 1119 [181] M. W. Gee, C. M. Siefert, J. J. Hu, R. S. Tuminaro, and M. G. Sala, “MI 5.0
1120 smoothed aggregation user’s guide,” Tech. Rep., 2006.
- 1121 [182] N. C. Reis Jr, J. P. De Angeli, A. F. de Souza, and R. H. Lopes, “Petroleum
1122 reservoir simulation using finite volume method with non-structured grids and
1123 parallel distributed computing,” 2001.
- 1124 [183] A. Datta-Gupta, J. Xie, N. Gupta, M. J. King, and W. J. Lee, “Radius of investi-
1125 gation and its generalization to unconventional reservoirs,” *Journal of Petroleum*
1126 *Technology*, vol. 63, no. 07, pp. 52–55 0149–2136, 2011.
- 1127 [184] J. Xie, C. Yang, N. Gupta, M. J. King, and A. Datta-Gupta, “Integration of shale-
1128 gas-production data and microseismic for fracture and reservoir properties with
1129 the fast marching method,” *SPE Journal*, vol. 20, no. 02, pp. 347–359
- 1130 [185] J. Xie, N. Gupta, M. J. King, and A. Datta-Gupta, “Depth of investigation and
1131 depletion behavior in unconventional reservoirs using fast marching methods,”
1132 2012.

- 1133 [186] Y. Zhang, C. Yang, M. J. King, and A. Datta-Gupta, “Fast-marching methods
1134 for complex grids and anisotropic permeabilities: Application to unconventional
1135 reservoirs,” 2013.
- 1136 [187] J. A. Sethian, *Level set methods and fast marching methods: evolving interfaces in*
1137 *computational geometry, fluid mechanics, computer vision, and materials science.*
1138 Cambridge university press, 1999, vol. 3
- 1139 [188] A. Datta-Gupta and M. J. King, *Streamline simulation: theory and practice.* So-
1140 ciety of Petroleum Engineers Richardson, 2007, vol. 11.
- 1141 [189] A. Datta-Gupta, J. Xie, N. Gupta, M. J. King, and W. J. Lee, “Radius of inves-
1142 tigation and its generalization to unconventional reservoirs,” 2011.